University of South-Eastern Norway
Faculty of Technology, Natural Sciences and Maritime Studies

Doctoral dissertation no. 68
2020

Thuy Thu Nguyen

Layer-specific strain and strain rate

Estimation using miniature transducers attached to the epicardium

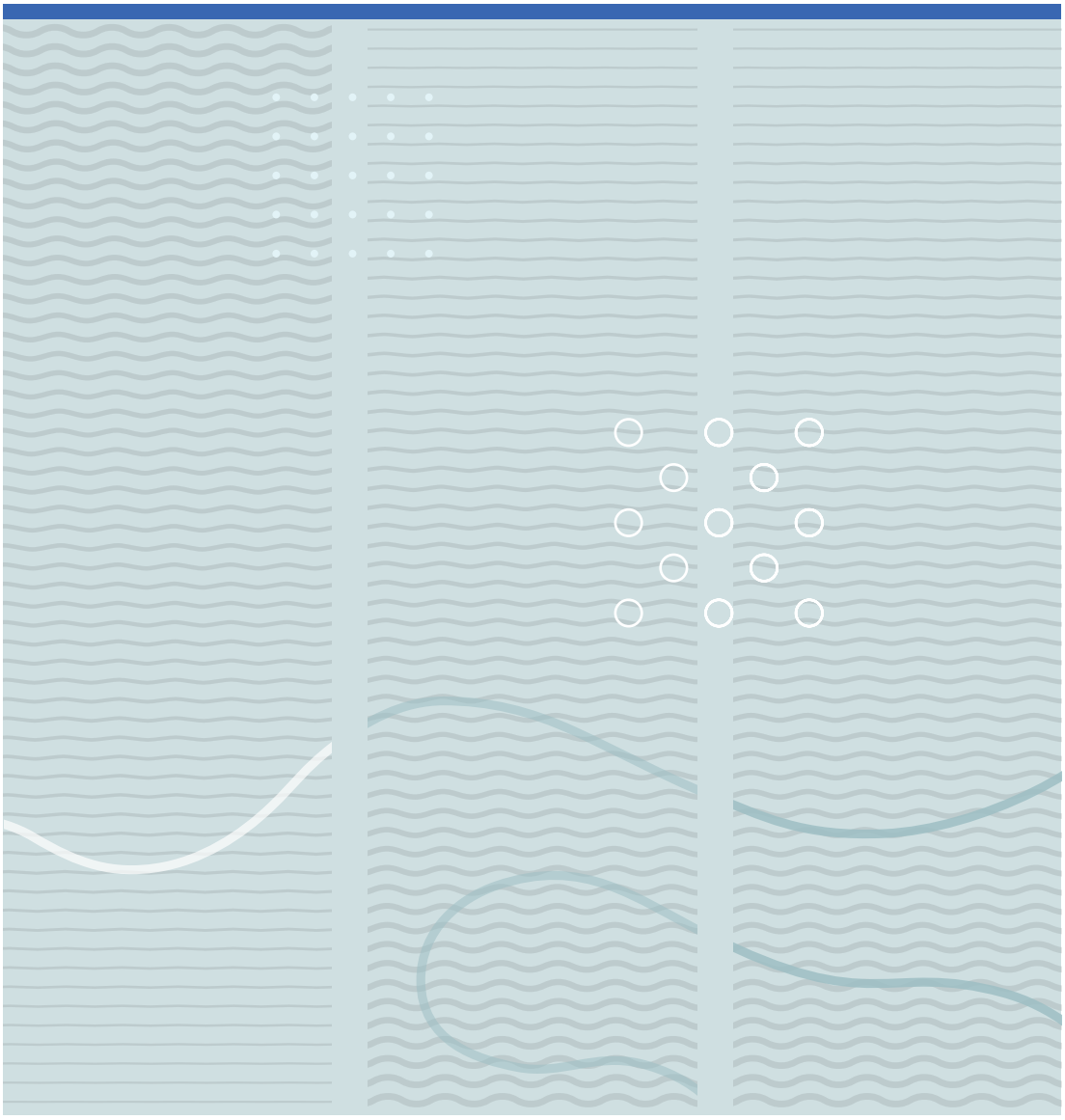

Thuy Thu Nguyen

Layer-specific strain and strain rate

Estimation using miniature transducers attached to the epicardium

A PhD dissertation in
Applied micro- and nanosystems

Faculty of Technology, Natural Sciences and Maritime Studies
University of South-Eastern Norway
Horten, 2020

Doctoral dissertations at the University of South-Eastern Norway no. 68
ISSN: 2535-5244 (print)
ISSN: 2535-5252 (online)

ISBN: 978-82-7860-429-8 (print)
ISBN: 978-82-7860-430-4 (online)

Print: University of South-Eastern Norway

Preface

This doctoral thesis is submitted in partial fulfillment of the requirements for the degree of Philosophiae Doctor at the Falculty of Technology, Natural Sciences and Maritime Sciences, University of Southeast Norway (USN), Norway.

The PhD work was carried out at the Department of Microsystems, Falculty of Technology, Natural Sciences and Maritime Sciences, University of Southeast Norway (USN), Norway under the supervision of professor Lars Hoff (USN), professor Jan D'hooge (KU Leuven), and dr. eng. Espen W. Remme (OUS).

Acknowledgment

First of all, I would like to express my sincere gratitude to my supervisors, professor Lars Hoff, professor Jan D'hooge, and dr.eng Espen W. Remme for the guidance and support during the years of my PhD study. Their positive attitude has always inspired my morale.

Professor Lars Hoff has offered me invaluable support. His insightful advices, patience, and encouragements have helped me to fulfill the research. Professor Jan D'hooge has given me fruitful guidance. I has gained valuable knowledge and was motivated after every discussion with him. Dr. eng. Espen W. Remme supported me greatly and was always willing to help me any time I need his support.

I would like to express my appreciation to dr. med. Andreas W. Espinoza and dr. med. Stefan Hyler for their great support in medical field.

I am grateful to the Department of Microsystems at University of South-Easten Norway for their useful facilities and administrative assistance. The Norwegian PhD Network on Nanotechnology for Microsystems is also deeply acknowledged for granting the travel supports to the internal conferences and for internship.

Last but not least, I must express my very profound gratitude to my father and to my husband for providing me with unfailing support and continuous encouragement throughout my years of study.

Abstract

Reliable methods to asses ventricular function during and after cardiac surgery are essential tools to evaluate patient prognosis. We presented an ultrasound system to monitor cardiac motion using miniature transducers attached directly to the epicardial surface. The aim is both as a research tool for detailed studies of cardiac mechanics, and to develop a continuous, real time system for perioperative evaluation of heart function. Two 3 mm diameter, 10 MHz ultrasound transducers were sutured to the epicardial surface. As the epicardial surface is the reference for the velocity and strain estimations, this procedure compensates for the motion of the heart. The short distance allows use of high frequencies and pulse repetition rates. The system was driven in pulse-echo mode, using electronics developed for the application, and RF-lines were recorded at pulse repetition rate 2500 s^{-1} and sampling rate 40 MS/s. This thesis presents the data processing methods used for heart disease diagnosis and in clinical research for the clinicians. We have categorized the work in this thesis into four main topics:

- Prove the feasibility of the measurement system in monitoring regional myocardial deformation.
- Look for suitable signal processing methods, especially velocity estimation methods with appropriate parameters for the specific measurement system.
- Build a simple simulation model in order to validate the data processing methods. The simulation model imitates the motion of the heart including contraction/expansion and rotation motions.
- Make the analysis tools available for clinicians and other researchers, to use in heart disease diagnosis.

The main contributions are:

- Feasibility of the measurement system in getting information about regional motion of myocardium was proved. This goal was achieved by employing the time delay estimation method to estimate tissue velocity and regional radial strain from experimental data recorded on animal models.

- The simulation model of insonified myocardium was built up and implemented it in Matlab (The MathWorks Inc., Natick, MA, USA). The axial deformation and rotation motion of the myocardium were considered in the simulation model. The graphic user interface was made to easily manage the input for the simulation, making the tool available for other researchers.

- The modifications of two standard velocity estimation methods (Time Delay Estimation (TDE) and phase shift Doppler methods) were presented. The methods were first tested in the simulation model and then on data from animal experiments. The evaluation of these methods was performed using Bland-Altman test between the results from the methods and the ground truth from the simulation model.

- The data processing method was implemented in Matlab (The MathWorks Inc., Natick, MA, USA). The Input and Output interfaces were supported to aid clinicians in entering the input parameters for data processing and analyzing and interpreting the output data, such as tissue velocity, radial strain, and myocardial layer tracking.

- The signal processing methods were applied ultrasound RF recordings on animal models, to test the feasibility of obtaining new clinical information, such as measurement of the transmural strain profiles at different sites inside myocardium of the left ventricle, and effect of myocardial perfusion on the end-systolic radial strain at the apex.

Symbols and Abbreviations

c	Speed of sound
ϵ	Lagrangian strain
ϵ_N	Natural strain
f_0	Center frequency
f_s	Sampling frequency
f_{prf}	Pulse Repetition frequency
λ	Wavelength
$L(t)$	Length at time instance t
R	Upsampling rate
T_{prf}	Pulse Repetition Time
V	Combination velocity
V_1	Velocity estimated from successive RF lines by TDE method
V_2	Velocity estimated from every second RF line by TDE method
$\hat{v}_{max}$	Maximum detectable velocity
$\hat{v}_{min}$	Minimum detectable velocity
RF	Radio Frequency
SD	Standard Deviation
SNR	Signal to Noise Ratio
TDE	Time Delay Estimation

Contents

List of Figures

List of Tables

Chapter 1

Introduction

1.1 Cardiac Mechanics - Background and Definitions

Myocardial motion is characterized along three principle components: longitudinal, circumferential and radial.These can be measured under normal closed chest conditions using a transthoracic ultrasound probe in an apical view, see Figure 1.1 (a). Delineation of the epicardium and endocardium is manually carried out, and real time analysis is difficult to achieve. An echocardiography study performed on 60 healthy adults showed slight regional heterogeneity in the circumferential strain, but not in longitudinal and radial strain [1]. Another study compared results from different ultrasound equipment manufacturers, software packages, frame rates, and observers [2], analyzing reproducibility for circumferential, radial and global longitudinal strain. The reproducibility between the different systems and observers was found to be good for global longitudinal strain, moderate for circumferential strain and poor for radial strain. Measuring radial strain observes the tissue along a line between the endo- and epicardial borders, covering around 10 mm thickness at end-diastole. Hence, measuring variations in velocity and strain within this distance requires data acquired at high spatial resolution, and radial strain is challenging to measure in transthoracic echocardiography. Moreover, short expansion or contraction phases may not be observed in close chest measurements due to the rotating motion of the heart during the cardiac cycle, and the limited frame rate allowed by the distance from the transducer to the region of interest. Some of these challenges can be mitigated during

open chest echocardiography, illustrated in Figure 1.1 (b). The shorter distance achieved by putting the ultrasound transducer directly onto the cardiac surface allows higher center frequency and pulse repetition rate, and the reduced attenuation improves the quality of the recorded data. One study [3] has indicated that circumferential strain could not be measured by placing the sensor on the heart's surface as a full short-axis image was very difficult to obtain, while it was possible to measure the longitudinal strain, being independent of angle. However, radial strain estimates showed high variance due to angle dependency. To avoid this problem, a silicon rubber was introduced between ultrasound probe and heart's surface and acted as a cushion for the heart motion [4, 5]. Using single element sewed on epicardium gives a chance to increase the center frequency, i.e. increase spatial resolution and to monitor heart's motion continuously.

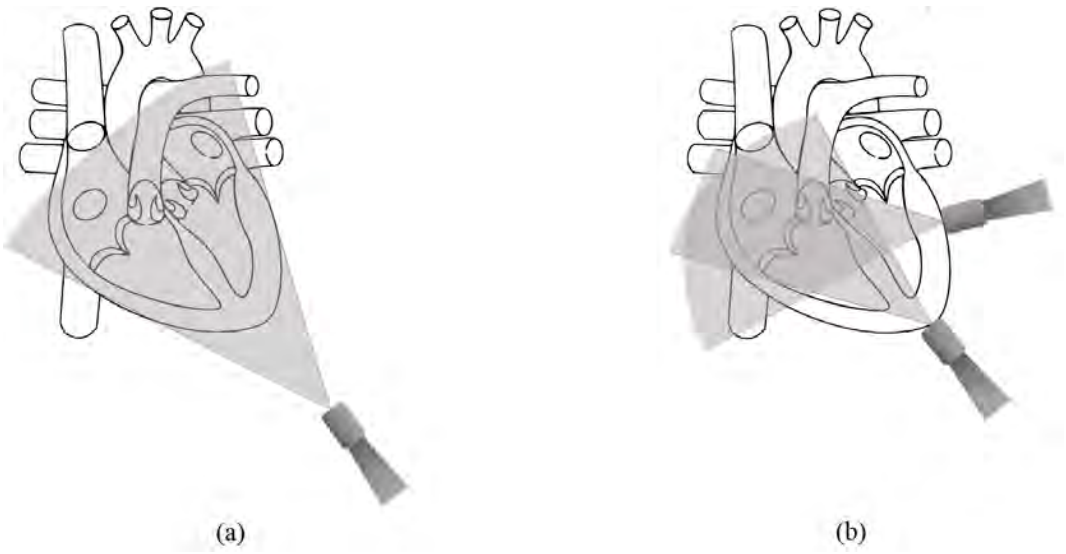

Figure 1.1: Schematic presentation of part of heart. The myocardium is insonated by an array transducer. (a) Closed chest. (b) Open chest with transducer placed on the heart's surface.

Ellis et al. [6] have showed how left ventricular diameter can be continuously measured by sonocardiometry, a technology using two or more two miniature ultrasonic transducers, denoted 'crystals', directly attached to the heart. In this technique, one crystal was used as a transmitter, and the other as receiver, and the method was used to measure local dimensional changes of the myocardium [7]. Hartley et al. demonstrated a method using one single-element transducer on the epicardium in a pulse-echo technique, to measure

myocardial thickening [8]. The myocardial deformation, represented by myocardial strain, reflects the work load of the myocardium, and the strain is therefore a suitable quantitative parameter characterizing the myocardial function [9–13]. Cardiac mechanics is complicated and is still not completely understood. For example, most studies of the distribution of radial strain across the left ventricular (LV) wall show increasing strain values from the epicardial layer to the endocardial layer [4], but there are also some that have show maximum strain in the mid-myocardium [14]. Computer models using the Finite Element Model to simulate the left ventricular contraction indicate that transmural fiber strain depends on the local curvature of the investigated segment [15, 16]. Moreover, some studies showed that there is a link between ischemia and changes in radial strain [5, 17]. Hence, detailed measurements of ventricular motion are of great interest to better understand the details in the heart mechanics, and may contribute to improve heart disease diagnosis.

1.2 Motivation and Hypothesis

According to the World Health Organization, ischemic heart disease is the major cause of death in the world, accounting for more than 16% of all deaths wold-wide in 2016 [18]. Hence, research into diagnosis and treatment of cardiac diseases is of high importance. The aim of this thesis is to develop new ultrasound-based monitoring methods to contribute to better treatment of cardiac diseases. The goals are two-fold: First, develop a new real-time monitoring system for continuous monitoring of cardiac function during cardiac surgery, and second, provide clinical researchers with a tool that can measure myocardial contractions in greater detail than possible with present methods.

We aim to achieve these goals by developing miniature, dedicated ultrasound systems to continuously monitor cardiac function during cardiac surgery, and possibly also during the first days following the surgery. The developed system should have faster response time and better sensitivity and specificity than ECG. The system is based on miniature ultrasound transducers attached directly to the epicardium, using a pulse-echo mode to monitor the motion of the layers inside the myocardium. The system should operate continuously for hours, in future versions perhaps even days, with minimal operator inter-

action. It should also be smaller, simpler and less expensive than conventional cardiac ultrasound scanners. The monitoring system has been developed over several years in collaboration between the University of South-Eastern Norway and Oslo University Hospital, Rikshospitalet [19–21]. Correct interpretation of the results requires appropriate algorithms for processing and presenting the data, and this is the central point of this thesis.

The main topic of the thesis is processing of RF signals acquired from this system. The goal is to develop algorithms for velocity and strain estimation and for tracking myocardial layers during the cardiac cycle. In the described studies, two miniature ultrasound transducers were mounted directly on the heart's surface, at two locations. The transducers were sutured to the epicardial surface during surgery, and removed before the chest was closed. However, future developments will aim for transducers small and smooth enough to allow them to be left on the heart after the thorax has been closed. In this case, e.g. a few days after surgery, when the risk of ischemia or other side-effects is reduced, the transducers can be removed by pulling them out through the thorax wall. Looking even further ahead, the principles developed in this project may also be used in implants for continuous monitoring of heart function. Since the transducers are attached to the epicardial surface, they move with the heart, thereby compensating for the heart's own movements. Such movements are a challenge in conventional transthoracic echocardiography, where the heart moves relative to the transducer, and parts of the myocardial tissue move in and out of the imaging plane. Furthermore, the short imaging depth allows higher frequency and higher pulse repetition frequency than with transthoracic echocardiography, allowing improved spatial and temporal resolution in the resulting velocity and strain values [22]. In addition to the ability to monitor heart motion real-time during surgery, the system is also intended as a tool for fundamental cardiac research, as the the detailed and continuously recorded motion data can provide new insight into the details of cardiac function.

The velocity estimators were based on two established estimation methods for ultrasound data: time delay estimation (TDE) and phase Doppler. In general, the time delay estimator is considered to perform better than the Doppler estimator [23–25], but requires more computations. The time delay estimator finds the time-shift based on cross-correlation

between successive echoes, i.e. a speckle tracking method, and calculates the velocity from this time-shift [26].

The accuracy of the *time delay estimator* depends mainly on the energy in the received echoes, and it is considered a robust estimation method [23–25]. In addition, using wideband excitation pulses can improve the range resolution and the accuracy of the velocity estimates [23]. TDE is not limited by aliasing, which can allow detecting higher velocities than pulsed Doppler, i.e. scatterer displacements larger than one wavelength per pulse repetition time [23]. A limitation of this method is the low velocity resolution, inversely proportional to pulse repetition time, and the high range resolution allowed by the short wideband pulses may in practice be limited by the kernel size. Furthermore, TDE can be time-consuming due to the large number of computations required. The one-dimensional TDE used in this study depends on insonation angle. The velocity resolution of TDE can be improved by either increasing the sampling rate or decreasing the PRF. The sampling rate can be synthetically increased by upsampling the RF scanlines before the estimator is applied, in the folowing denoted *TDE with upsampling*. This will smoothen the curves and may improve the accuracy of the estimator, at the cost of a requiring a higher number of computations. TDE will have problems detecting velocities where the displacement between successive scanlines is smaller than one sample. This can be mitigated by omitting some scanlines and combining every second, third, etc. scanline, corresponding to reducing the PRF of the received echoes. Relative to the epicardial surface, different myocardial regions move at very different velocities: The motion is normally slow close to the epicardial surface and increases towards the endocardial wall. This puts different requirements to the velocity estimator depending on the depth into the myocardial wall: High velocity resolution is wanted in the slow-moving regions close to the epicardial surface, while high maximum velocity is wanted in the faster moving regions close to the endocardial wall. To satisfy these varying requirements, we propose to process the scanlines differently depending on the depth into the myocardium, using a modified TDE, *TDE with velocity combination*. In this scheme, tissue velocities in slow motion regions are estimated omitting some of the RF scanlines, correlating every second, third or fourth scanline, while velocities in the faster motion regions are calculated by correlating every

scanline.

Pulsed Doppler velocity estimators are limited by aliasing, requiring the scatterer displacement between two successive pulses to be less than a half a wavelength, or equivalently, the phase difference between two consecutive scanlines must be less than π. This puts a maximum to the detectable velocity [23, 26]. The Doppler method is computationally fast [25], but susceptible to noise [23–25]. The phase shift Doppler method depends on the center frequency of the echoes. Myocardium is a strongly attenuating tissue [27], and its thickness changes over the cardiac cycle. The myocardium is also anisotropic, with a frequency-dependent attenuation coefficient that depends on the orientation of the acoustic axis relative to the muscle fibers. As a result, the center frequency of the received signals is a function of depth and time. The phase Doppler is a one-dimensional velocity estimator, depending on the insonation angle [26, 28]. The velocities are estimated from frequency shift [23], and the accuracy degrades when wide bandwidth excitation is employed, hence, long pulses are required. As for the time delay estimator, we also propose a modification to the phase shift Doppler to better handle the large velocity variations found in the myocardium. The conventional phase shift Doppler [26] (*constant velocity Doppler*) assumes constant velocity within each pulse packet. To allow for rapidly changing velocities, the method was extended by allowing constant acceleration within each pulse packet, and the velocity formula was modified accordingly. This modified method was denoted *constant acceleration Doppler*. It can be beneficial in regions where tissue velocities change rapidly, as it allows velocities to vary linearly versus time within each packet.

Attaching the ultrasound transducers to the heart's surface allows high PRF due to the short depth of image and improves recorded data quality by reducing noise. The bandwidth of the emitted pulses was 60% of the center frequency, giving a pulse length of three and a half wavelengths. We hypothesize that the constant acceleration Doppler method improves velocity estimates from the faster moving regions close to the endocardium, and that the velocity resolution from the TDE can be improved by either upsampling RF data before processing, or by processing different RF-line combinations depending on depth.

The proposed modifications were evaluated by using data from a simulation model, with three different settings, and real data from animal experiments. Furthermore, two pilot studies on heart mechanics were done using the measurement system and the new processing algorithms, testing if our method may provide new insight into two still not fully known phenomena: Variation of radial strain along the myocardial thickness, and specifically whether this distribution depends on the local curvature of the myocardium, and change in radial strain in the different myocardial layers under various level of reduced blood supply. These studies must be regarded as preliminary with the intention to demonstrate capabilities of the system and methods, and no clinical conclusions should be drawn from them.

Based on this, the goals of this project are defined as

- Investigate whether the system with two epicardial transducers can monitor myocardial motion continuously
- Estimate radial velocity, strain rate, and strain in different transmural layers, from the epicardium to the endocardium
- Compare results from a computationally light pulse Doppler method to results from a time delay estimator. Compare result quality and processing time.
- Investigate improved velocity estimators to better capture the large span in velocities expected in the myocardium: Slow in the sub-epicardium and faster close to the endocardium
- Develop a myocardial simulation model to test the estimators
- Test the estimators on real data acquired from animal experiments.

Chapter 2

Materials and Methods

2.1 Transducer, Electronics and Data Acquisition

Figure 2.1 shows schematic illustration of the main parts of the measurement system. The system contains a two-channel ultrasound transmit-receive system built in-house from state of the art electronic components. The system employed custom-build single-element transducers (Imasonic SAS, Besancon, France). The transducers have 3 mm active diameter, center frequency 10 MHz, 60% bandwidth, and are focused geometrically to 20 mm. The two ultrasound transducers were excited concurrently, and the received echoes from these two transducers were divided into two separate receive channels in the transmit/receive switch. The transducers were mounted so that the distance between them was larger than twice the maximum imaging depth, ensuring that the receiving was finished before the direct wave from one transducer reached the other to avoid interference between the two transducers. The received echoes were digitized at 40 MS/s, and stored on a memory disk. The pulse repetition rate is 2500 pulses/s. ECG and three blood pressures were registered and synchronized with the ultrasound measurements, to provide time references for the cardiac cycle. The locations of the three pressure catheters depended varied between on each the experiments, but in most many cases, they were placed in the aorta, left ventricle and left atrium.

2.2 Animal Experiment Procedure

The ultrasound system was tested in open chest porcine experiment. The ultrasound recording was obtained in a study previously published [29]. The use of animals in that study was approved by National Animal Research Authority in Norway (No. 27/09-1747). The handling of the animals was in accordance with institutional guidelines, and national and international regulations. The re-use of the recordings in this study is in accordance with the Three R's, to reduce the number of animals used in research [30]. Two sensors were sutured to the epicardial surface of the left ventricle. One transducer was placed in the apical region, near the intervention area, and one in the basal region, far from the intervention area, as shown in Figure 2.2. Wobbling of the transducer during the heart cycle may cause myocardial tissue move in and out of the insonified area, causing artifacts. To minimize this, the transducers were mounted at positions with minimal angular motion of the epicardial surface. However, this was done by visual judgements only, no quantitative assessment of this was done.

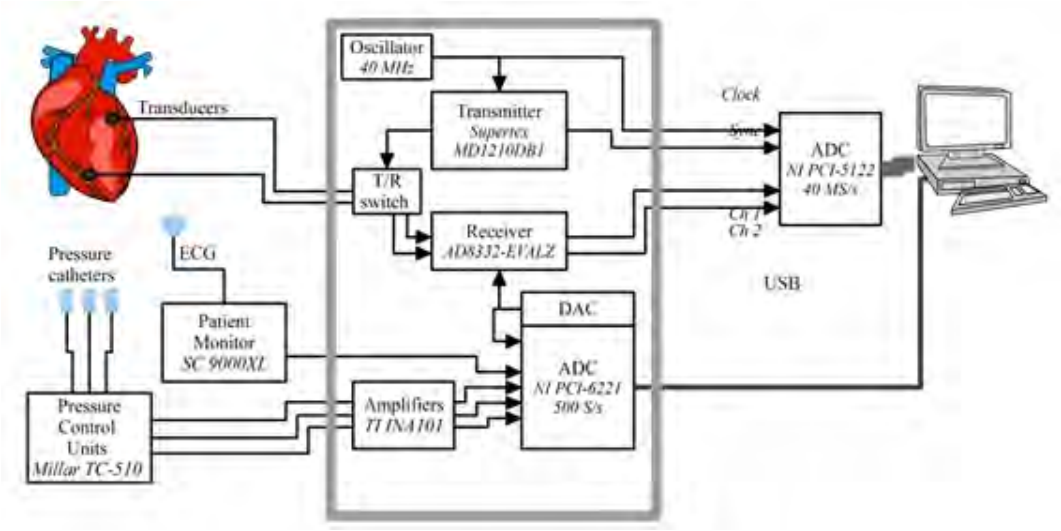

Figure 2.1: Schematic illustration of the main parts of the measurement system. Two transducers sutured to the heart are connected to the analog ultrasound transmit-receive system. The signals from this system are digitized and transferred to a computer. ECG and pressure catheter signals are sampled simultaneously, and synchronized with the ultrasound recordings using pulses from an analog output (DAC). ADC = analog to digital converter; Ch = channel; DAC = digital to analog converter; ECG = electrocardiography; Sync = synchronize; T/R switch = transmit-receive switch; USB = universal serial bus.

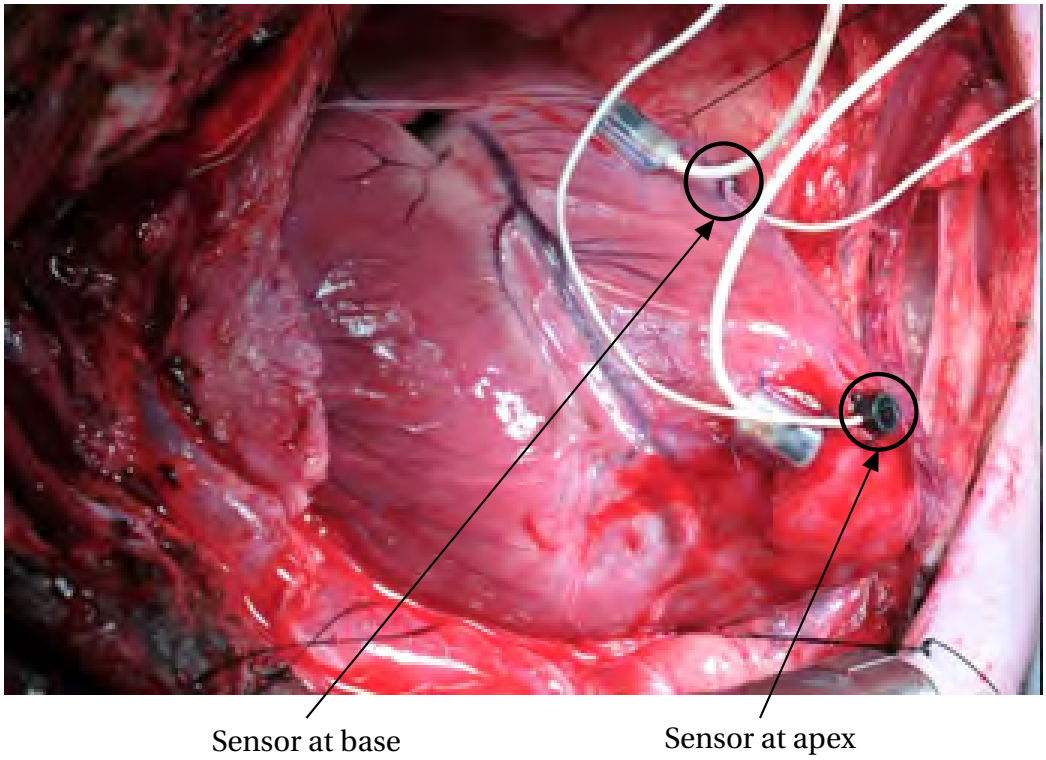

Figure 2.2: Image of transducers sutured to a pig heart. Two transducers were sutured to the heart surface: one in the apical region, one in the basal region. In order to reduce the number of animal experiments, the experimental protocol also included attachment and testing of accelerometer sensors, as part of a different study.

2.3 Velocity and Strain Estimation Methods

2.3.1 Strain and Strain Rate

The myocardial deformation during contraction and relaxation occurs in all directions. The myofibrils are shortening in their length direction during contraction, and thickening across the transverse direction. As the muscle fibers in the cardiac wall are arranged in longitudinal, oblique and circumferential directions, the contraction results in shortening of the cardiac wall in longitudinal and circumferential directions. Wall thickening occurs throughout the cardiac wall as a result of the shortening across several directions. During relaxation the ventricular cavity is filled with blood and the myofibrils are stretched and the diameter is reduced, resulting in lengthening and thinning of the cardiac wall. Strain is defined as relative deformation of a body, normalized to its original shape. A single element transducer was used in the ultrasound measurement system. We therefore focus

on radial strain in the myocardium. The thickness of myocardium is increased during the ejection phase, and decreased during the filling phase. The *Lagrangian strain* ε, the instantaneous strain during deformation, is defined by[11]

$$\varepsilon(t) = \frac{L(t) - L(t_0)}{L(t_0)} \tag{2.1}$$

where $L(t_0)$ is the length of the object at initial time t_0 and *L(t)* is the length of the object at time *t*. The *natural strain* ε_N is defined as the integral of infinitesimal strain occurring during an infinitesimal time interval, i.e. the total strain during the whole deformation process

$$\varepsilon_N(t) = ln\frac{L(t)}{L(t_0)} \tag{2.2}$$

By combining (2.1) and (2.2), the relationship between *Lagrangian strain* and *natural strain* is expressed as

$$\varepsilon(t) = exp(\varepsilon_N(t)) - 1 \quad \text{or} \quad \varepsilon_N(t) = ln(\varepsilon(t) + 1) \tag{2.3}$$

Consider a bar with length $L(t)$ at time t and length $L(t + dt)$ at time $t + dt$ in Figure 2.3. Then the *strain rate* $\dot{\varepsilon}_N(t)$ is defined as the time derivative of the natural strain ε_N

$$\dot{\varepsilon}_N(t) = \frac{d\varepsilon_N(t)}{dt} = \frac{v_2 - v_1}{L(t)} \tag{2.4}$$

where v_1 and v_2 are the velocities of scatterers at the left and right boundaries of the bar. This is the basis for finding the strain rate in the myocardium from variations in velocity as function of radial distance. It is evident from (2.4) that the quality of the strain estimates is affected by the quality of velocity estimates. The velocity estimates in our studies are taken from ultrasound recordings using e.g. time delay or phase shift Doppler estimators.

2.3.2 Velocity from Time Delay Estimation (TDE)

The time delay between two sequential radio frequency (RF) signals $r_{s1}(t)$ and $r_{s2}(t)$ is determined by checking the similarity of reflected RF waveforms. The time delay is defined

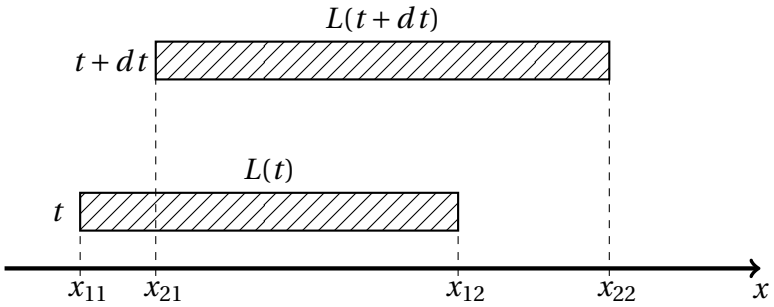

Figure 2.3: Deformation of a bar during infinitesimal time dt. The bar has the length of $L(t)$ at time t, length of $L(t+dt)$ at time $t+dt$.

as time lag t_s of the most similar waveforms within two windows, see the example in Figure 2.4. The window length in denoted the kernel size. Increasing the kernel size reduces the noise in the measured values, at the cost of reduced axial resolution. Cross-correlation is a common and accurate method to measure the similarity between two signals. The cross-correlation function between two signals $r_{s1}(t)$ and $r_{s2}(t)$ is [26]

$$R_{12}(\tau) = \frac{1}{2T}\int_T r_{s1}(t)r_{s2}(t+\tau)dt \tag{2.5}$$

The time delay t_s is determined by the position of the maximum of $R_{12}(\tau)$. When the RF signals are sampled, the cross-correlation function between two discrete signals $r_{s1}(k)$ and $r_{s2}(k)$ becomes:

$$\hat{R}_{12}(n, i_{seg}) = \frac{1}{N_s}\sum_{k=0}^{N_s-1} r_{s1}(k+i_{seg}N_s)r_{s2}(k+i_{seg}N_s+n) \tag{2.6}$$

where N_s denotes the number of samples in the segments, and i_{seg} is the segment number. The accuracy of the estimate can improved by interpolating between the samples, using a parabolic interpolation [26, 31]. If the position of the maximum of $\hat{R}_{12}$ is found at n_p, the parabolic fit uses the values of this point $\hat{R}_{12}(n_p)$ and its neighbours $\hat{R}_{12}(n_p-1)$ and $\hat{R}_{12}(n_p+1)$ to estimate the interpolated maximum position n_{int} as

$$n_{int} = n_p + \frac{\hat{R}_{12}(n_p-1) - \hat{R}_{12}(n_p+1)}{2\left(\hat{R}_{12}(n_p-1) - 2\hat{R}_{12}(n_p) + \hat{R}_{12}(n_p+1)\right)} \tag{2.7}$$

The velocity estimate $\hat{v}$ is found from the shift in position n_{int} between the scanlines as

$$\hat{v} = \frac{c}{2} n_{int} \frac{f_{prf}}{f_s} \tag{2.8}$$

where f_{prf} is pulse repetition frequency f_s is the sampling frequency, and c is the speed of sound in the medium. The maximum detectable velocity of this method is

$$\hat{v}_{max} = \frac{c}{2} N_s \frac{f_{prf}}{f_s} \tag{2.9}$$

A shift of one sample point between successive scanlines can be taken as a minimum for a reliable detection of velocity. However, due to the interpolation, this is not a hard limit for the minimum detectable velocity. The velocity corresponding a shift of one sample point is

$$\hat{v}_{min} = \frac{c}{2} \frac{f_{prf}}{f_s} \tag{2.10}$$

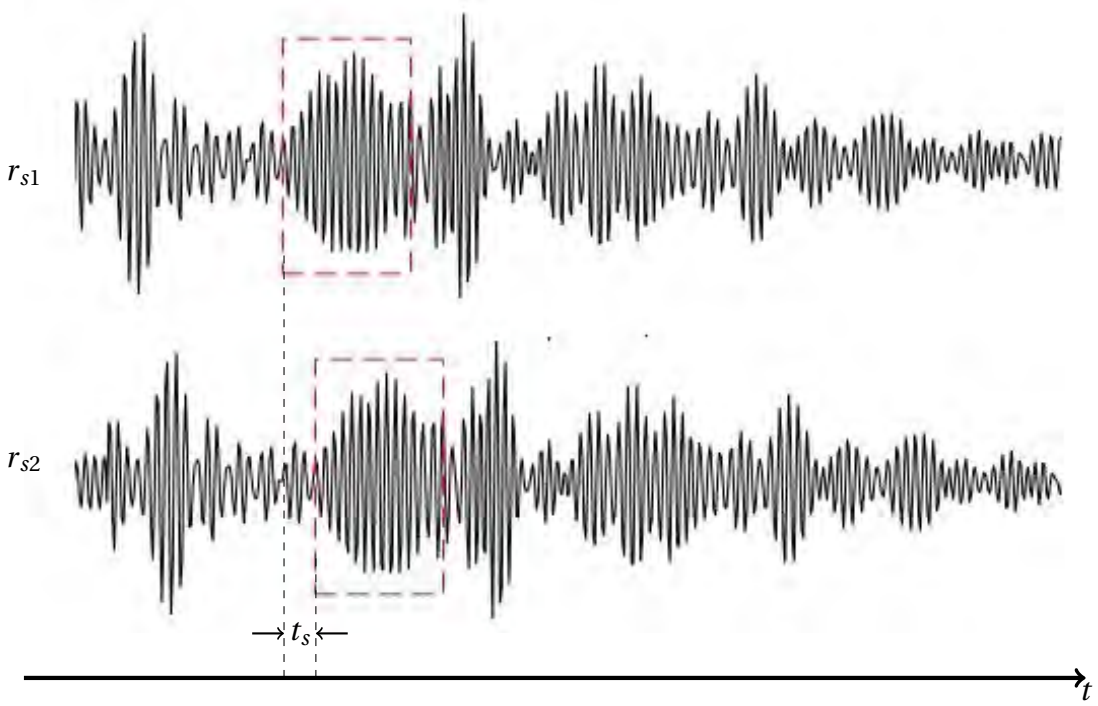

Figure 2.4: The waveform of two RF scanlines r_{s1} and r_{s2}. The time delay between two sequential RF signals $r_{s1}(t)$ and $r_{s2}(t)$ is determined by time shift between two patterns within windows marked in dashed red line.

The velocity resolution was improved either by upsampling the scanlines before applying

the cross-correlation, which increases f_s, or by processing every 2nd, 3rd or 4th scanline, which reduces f_{prf}. The resolution in the calculated velocities was further improved by applying parabolic sub-sample interpolation to find the maximum in the cross-correlation curves. When quantitatively comparing the TDE methods, we have chosen to compare the minimum and maximum velocities before sub-sample interpolation, as these are well-defined numbers suitable for comparison.

The tissue velocity will in general increase with the depth, i.e. the sub-epicardial tissue usually moves at higher speed than the sub-endocardial tissue. Hence, the requirements to the velocity estimator are different in the different regions of the myocardium: The sub-epicardium requires better velocity resolution but not as large maximum detectable velocity as the sub-epicardium. In order to balance these requirements, the RF lines can processed differently depending on depth [12]. This modification to the TDE, denoted *TDE with velocity combination*, finds the velocity $V(z)$ at depth z from a combination of two velocity estimates V_1 and V_2. In the present study, we have extended this method further by introducing two additional velocity components V_3 and V_4 computed from cross-correlation between every third and fourth scanline

$$V(z) = \begin{cases} V_4, & z < z_3 - d \\ \frac{z-z_3-d}{d}(V_3 - V_4) + V_4, & z_3 - d \leq z \leq z_3 \\ V_3, & z_3 \leq z \leq z_2 - d \\ \frac{z-z_2-d}{d}(V_2 - V_3) + V_3, & z_2 - d \leq z \leq z_2 \\ V_2, & z_2 \leq z \leq z_1 - d \\ \frac{z-z_1-d}{d}(V_1 - V_2) + V_2, & z_1 - d \leq z \leq z_1 \\ V_1, & z > z_1 \end{cases} \tag{2.11}$$

where the velocity V_1 is calculated from the cross-correlation between successive scanlines, V_2 from the cross-correlation between every second scanline, V_3 between every third, and V_4 between every fourth scanline. This means that for V_2, half of the RF data are neglected, V_3 processes one third of the RF data, and V_4 processes one fourth of the data.

The parameters z_3, z_2, and z_1 are determined by comparing the velocities V_k , k=1,2,3,4 with the maximum detectable velocity using this estimator [32]. The minimum detectable velocities before sub-sample interpolation using V_3 and V_4 were 32 mm/s and 24 mm/s, respectively. The transition regions d are fixed to 1 mm.

Another approach tested to increase the velocity resolution from TDE was upsampling RF scanlines before the cross-correlation, *TDE with upsampling*. The upsampling factor R was chosen to $R = 10$. This reduces the minimum detectable velocity by the same factor, to 4.8 mm/s if all scanlines are compared. The maximum shift allowed by the TDE estimator was limited to half a wavelength, as explained in the Introduction. This limited the maximum detectable velocity, but also reduced the calculation time. The cross-correlation calculations were done in Matlab by forming a matrix containing the first scanline and all possible shifts of the second scanline, reducing calculation time compared to calculating all results in sequence, approximately 1.5 times faster.

The velocities in (2.6) and (2.8) were estimated based on an assumption that the scatterers only traveled in axial direction. The precision of the time shift estimate was derived by Embree [33] and Foster et al.[34]. The standard deviation (SD) of the estimated time shift is [26]

$$\sigma[t_s] = \frac{\sqrt{2}}{B_{rms}\sqrt{\frac{E}{N_0}}(1 - 1.2|v|T_{prf}sin(\theta)/b_{3dB})} \tag{2.12}$$

where B_{rms} is the root mean square bandwidth of the received RF signals [rad/s], E is the energy of the received echoes reflected from one pulse emission [J], and N_0 is the power density of additive white noise [W/Hz]. θ is the insonation angle, v is velocity of scatterer, and b_{3dB} is the 3dB beamwidth.

From (2.12), it can be seen that the accuracy of the time shift estimate can be improved by increasing the bandwidth of the ultrasonic transducer, the signal to noise ratio ($\frac{E}{N_0}$), reducing the insonation angle θ, or increasing the pulse repetition frequency $f_{prf} = 1/T_{prf}$.

2.3.3 Velocity from Phase Shift Doppler

As an alternative to the time delay estimator, TDE, velocities can also be found from the pulse Doppler method. The Doppler method described in this section refers mainly to theory described by Jensen [26]. The Doppler effect is a well-known phenomenon from everyday experience, causing the frequency to change when a receiver moves relative to the source, or, as the case in these studies, when waves are scattered from a moving object. The emitted pulses are scattered from moving scatterers and received by the same stationary ultrasound transducer. The received RF signal from pulse number i emitted at time t is [26]

$$r_{si}(t) = a \cdot e(\alpha_i(t - t_0) - t_{si}) \tag{2.13}$$

where $e(t)$ is the shape of the emitted pulse, a is the scatterer strength, and t_0 is time from emission to reception, given by

$$t_0 = \frac{2d_0}{c - v_1} \tag{2.14}$$

Here, d_0 is the position of the scatterer at initial time t = 0, and v_i is the scatterer's velocity along the acoustic beam at the time when the ith pulse was emitted, and α_i is the pulse compression factor from the scatterer motion at the time of interaction with the ith acoustic pulse

$$\alpha_i = \frac{c - v_i}{c + v} \approx 1 - \frac{2v_i}{c} \tag{2.15}$$

The approximation is valid as the tissue velocity is always much smaller than speed of sound, i.e. $v_i \ll$c. t$_{si}$ is the time shift from scatterer movements between the first and the ith emitted wave

$$t_{si} = 2\frac{T_{prf}}{c}\sum_{k=0}^{i-1}\bar{v}_k \tag{2.16}$$

The emitted pulse is described as a sine wave enclosed in a window function g(t), typically lasting a few cycles [26]

$$e(t) = g(t)sin(2\pi f_0 t) \tag{2.17}$$

The simplest shape for the window function g(t) is a rectangular window of length M cycles

$$g(t) = \begin{cases} 1, & 0 < t < \frac{M}{f_0} \\ 0, & \text{elsewhere} \end{cases}$$

After demodulation with frequency f_0, the received signal becomes:

$$s_{oi}(t) = a \cdot g_i(t) sin(2\pi f_0[(\alpha_i - 1)t - t_{si}]) \tag{2.18}$$

$$g_i(t) = g(\alpha_i(t - t_0) - t_{si}) \tag{2.19}$$

The common assumption in ultrasound pulse Doppler estimates in setting the velocity v_i within a packet to be a constant v. To distinguish this from other models tested in this thesis, we call this (*constant velocity Doppler*). In this case, the i$^{\text{th}}$ demodulated signal becomes

$$s_{oi}(t) = a \cdot g(t) sin\left(2\pi f_0 \left[-\frac{2v}{c}t - \frac{2v}{c}(i-1)T_{prf}\right]\right) \tag{2.20}$$

This expression for $s_{oi}(t)$ in (2.20) is identical to the one derived by Jensen [26].

Assuming constant velocity within each Doppler pulse packet can be a limitation. This model can be extended by adding a constant acceleration factor to the velocity formula over a pulse packet (*constant acceleration Doppler*), expressing the velocity v_i as

$$v_i = a_1 i + a_0 \tag{2.21}$$

The i$^{\text{th}}$ demodulated signal is simplified by substituting (2.15) and (2.20) into (2.18), giving

$$s_{oi}(t) = a \cdot g(t) sin\left(\frac{2\pi f_0}{c}\left[a_1 T_{prf} i^2 - 2(a_1 t + a_0 T_{prf})i + a_1 T_{prf} + 2a_0 T_{prf}\right]\right) \tag{2.22}$$

The tissue velocity is hence estimated by fitting the phase of demodulated signal to the second order polynomial.

The difference in phase between two successive elements in a packet must be smaller

Table 2.1: Parameter settings for velocity estimation methods

Estimation method	Parameter	Value	Unit
Constant velocity Doppler	Packet size for estimation	4	pulse
and	Sample volume for $\hat{f}_0$	4	λ
Constant acceleration velocity	Packet size for $\hat{f}_0$	4	pulse
	Cutoff frequency for $\hat{f}_0$	14	MHz
TDE	Upsampling rate	10	
	Kernel size	4	λ
	Window overlapping	50	%

or equal to π. (2.20) results in the maximum detectable velocity for constant velocity Doppler:

$$v_{max} = \frac{cfprf}{4f_0} = 96mm/s \tag{2.23}$$

The Doppler estimators require therefore high PRF to avoid aliasing in velocity estimation while TDE is not restricted by this limit. Table 2.1 shows parameters phase Doppler and TDE estimators used in the thesis.

2.4 Simulation Model for Cardiac Contraction

A simple simulation model was built up in order to test and verify the data processing method in a controlled environment. The model was used to simulate controlled motion patterns inside the myocardium. The received RF scanlines were generated using the software package Field II [35, 36]. The parameters used in the simulation are listed in Table 2.2. Additive random Gaussian noise was introduced to the echoes to investigate the influence of noise on the velocity estimates. The noise level is quantified by the signal to noise ratio (SNR).

The illuminated myocardium is modelled as a rectangular cuboid. The parameters of the transducer and the dimensions of the simulated myocardium are listed in Table 2.2. The myocardial motion was described by two basic constituents, contraction and rotation. The contraction was represented by radial velocity $v_z(x,y,z,t)$. The transducer area was small, giving a narrow beam illuminating a small part of the myocardium. Lateral

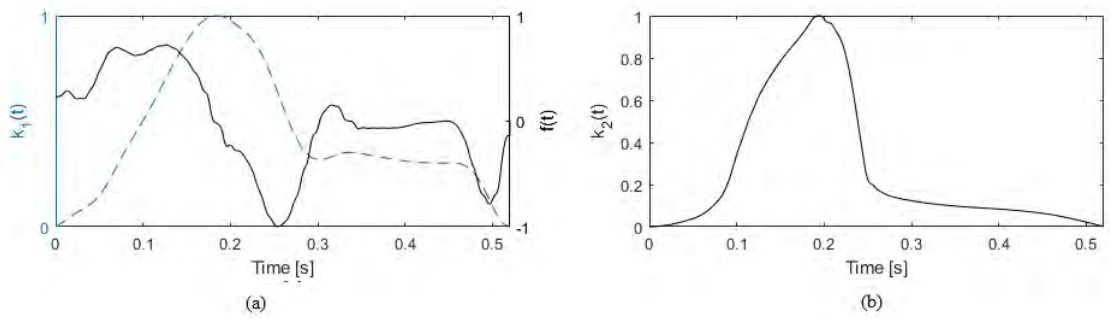

Figure 2.5: Simulation model for myocardial contraction and rotation motion over one cardiac cycle. Normalized compression $k_1(t)$ as function of time (dashed blue line), and its normalized derivative dk_1/dt (solid black line) (a), normalized left ventricular torsion as function of time $k_2(t)$ (b).

variations in the radial velocity within this beam were neglected, hence, the tissue velocity was described as a function of two independent variables, depth z and time t. Under this assumption, the velocity could be described as a product of a function of depth $g(z)$ and a function of time $f(t)$

$$v_z(z,t) = g(z) \times f(t) \tag{2.24}$$

The motion of the simulated myocardium was realized based on two parameters k_1 for contraction and k_2 for rotation motion from the kinematic model [37, 38], where k_1 is the radially dependent compression and k_2 is the left ventricular torsion shown in Figure 2.5. The normalized derivative of k_1 was used as model for the time variation $f(t)$ shown in Figure 2.5a. The depth variation $g(z)$ was modeled as a 2^{nd} order polynomial as function of depth given in Table 2.2.z is the distance from the transducer into the myocardium, measured in meters.

The myocardium model was evenly meshed into elements initial time. Positions of meshing nodes versus time were calculated under radial deformation and rotation using formulas in *Paper B*. The scatterers were then filled into the myocardium with the density given in Table 2.2 . The sampling frequency in the simulation was set 200 MHz in order to avoid aliasing, and the RF signals from simulation were then down-sampled from 200 MHz to 40 MHz, to be consistent with the experimental recordings. The RF data from the

Table 2.2: Parameter settings for simulation.

Parameter	Value
Scatterer density	1.875×10^{12} m^{-3}
Attenuation coefficient, frequency dependent	0.71 cm^{-1} MHz^{-1}
End-diastolic myocardium dimensions	4 mm x 4 mm x 10 mm
Meshing grid	0.2 mm x 0.2 mm x 0.25 mm
Transducer aperture radius	1.5 mm
Transducer curvature (spherical focal radius)	20 mm
Speed of sound in tissue	1540 m/s
Transmit pulse center frequency (f_0)	10 MHz
Sampling rate used in Field II	200 MHz
Transmit pulse length	400 ns
g(z)	520 z^2
Signal-to-noise ratios	3dB, 5dB, 10dB, 15dB, 20dB and 40dB

Table 2.3: Parameter settings for three different myocardial motion patterns in simulation

Parameter	Simulation 1	Simulation 2	Simulation 3
g(z)	520z^2 (m)	480z^2 (m)	-50z^2+6z (m)
Maximum rotation angle α	3^0	5^0	5^0

z is the distance from the transducer into the myocardium, measured in meters.
$g(z)$ is a shape function modelling the variation in myocardial velocity with depth, with unit meter.

simulation at different SNR levels in Table 2.2 were investigated in order to evaluate the accuracy of velocity estimation methods. Three different myocardial contraction patterns, represented by the three different versions of $g(z)$, and maximum tilt angle in Table 2.3 were tested in the simulation model.

Chapter 3

Research Goals and Tasks

3.1 Research Goals

This thesis aims at a better interpretation of the signals received from a system using miniature ultrasound transducers attached directly to the epicardial surface. The main task is to develop new processing algorithms for the RF scanlines to find velocity and strain and for tracking of myocardial layers. Compared to conventional transthoracic imaging, epicardially mounted ultrasound transducers opens new opportunities. First, the transducers move with the heart, compensating for the heart's own movements. Moreover, the imaging depth is shortened and the sound does not need to travel through the chest wall. This allows higher center frequency and higher pulse repetition frequency, improving spatial and temporal resolution. The intended application of the results is two-fold. We aim at developing technology for a tool for continuous monitoring of cardiac function. In addition, we believe the developed methods have an unique ability to provide detailed information about contraction/expansion in the different layers of the myocardium, hence, providing a research tool to explore a topic of great interest in basic cardiology research.

Hypotheses to be investigated in this work are

- Regional myocardial motion can be measured and monitored using the described measurement system and the algorithms for velocity estimation and layer tracking developed in the project.

- Using the constant acceleration Doppler method will improve the ability to capture details in the velocity patterns, compared to conventional constant velocity Doppler.
- Velocity estimates from the time-delay estimator (TDE) can be improved by either upsampling the RF scanlines before applying the TDE, or by using the TDE with a velocity combination algorithm.

The research goals of the project are defined as

- Develop, test and compare different velocity estimators applied to signals from the epicardially mounted transducers. The following two classes of estimators should be compared
  - Phase-shift Doppler methods.
  - Time-delay estimators.
- Use the resulting velocity fields to estimate strain and stain rate.
- Use the resulting velocity fields to track myocardial motion through one heart cycle.
- Test the algorithms on a simulation model for cardiac contractions.
- Test the algorithms on real RF data recorded from animal studies.
- Apply the results to selected test-cases of interest in cardiac research.
- Implement the algorithms in well-documented and user-friendly Matlab programs.

3.2 Tasks

In order to reach the goals listed above goal, the following tasks must be achieved:

- Prove feasibility of the measurement system in monitoring regional myocardial motion.

- Look for signal processing methods, especially velocity estimation methods, for the specific measurement system in Figure 2.1 to extract information about the heart's motion in details, either towards a clinical tool and/or as a research tool for basic clinical research.
- Build a simple simulation model which imitates the translation and rotation motion of insonified part of myocardium. The simulation model is then used to evaluate the velocity estimation methods. The evaluation is based on criteria of accuracy and computation time.
- Obtain data from real animal studies, and test methods on the experimental data.
- Make the methods available for clinicians, used in heart disease diagnosis and in clinical research.

Chapter 4

Summary of Results Achieved

The 10 MHz transducers attached directly to the myocardium gave low noise raw data of sufficient resolution in space and time to allow reliable tracking the motion of the myocardial layers. It was demonstrated that this measurement system can be used to track myocardial deformation and study regional myocardial strain. The velocity estimates found from these raw RF scanlines are the basis for the following calculations. Hence, robust velocity estimators are essential for all further computations such as layer tracking strain rate and strain estimates. The conventional velocity estimation methods (TDE and phase shift Doppler methods) and their modifications were evaluated using data from the simulation and animal model. All measurements in this thesis were made with the chest open. The heart motion is in this situation not identical to when the chest is closed, and this may also influence the strain patterns inside the heart muscle. This must be borne in mind when interpreting the results

A fifth median filter along the time was applied to velocities estimated by Doppler-based estimator. The bias and standard deviation (SD) of the difference between the estimated data (velocities and strains) and the true values from the simulation model are shown in Figure 4.1. The maximum simulated velocity and strain were approximate 96 mm/s and 72%, and the thickness of each myocardial layer at end-diastole was 1.5 mm. The bias and SD for all layers lumped together were very similar for the constant velocity Doppler and the constant acceleration Doppler estimators, see Figure 4.1a and 4.1b. The constant ac-

celeration Doppler showed slightly lower bias and SD than the constant velocity Doppler for all investigated SNR values, for both the velocity and strain estimates, but this differences were too small to be regarded remarkable. The constant acceleration Doppler

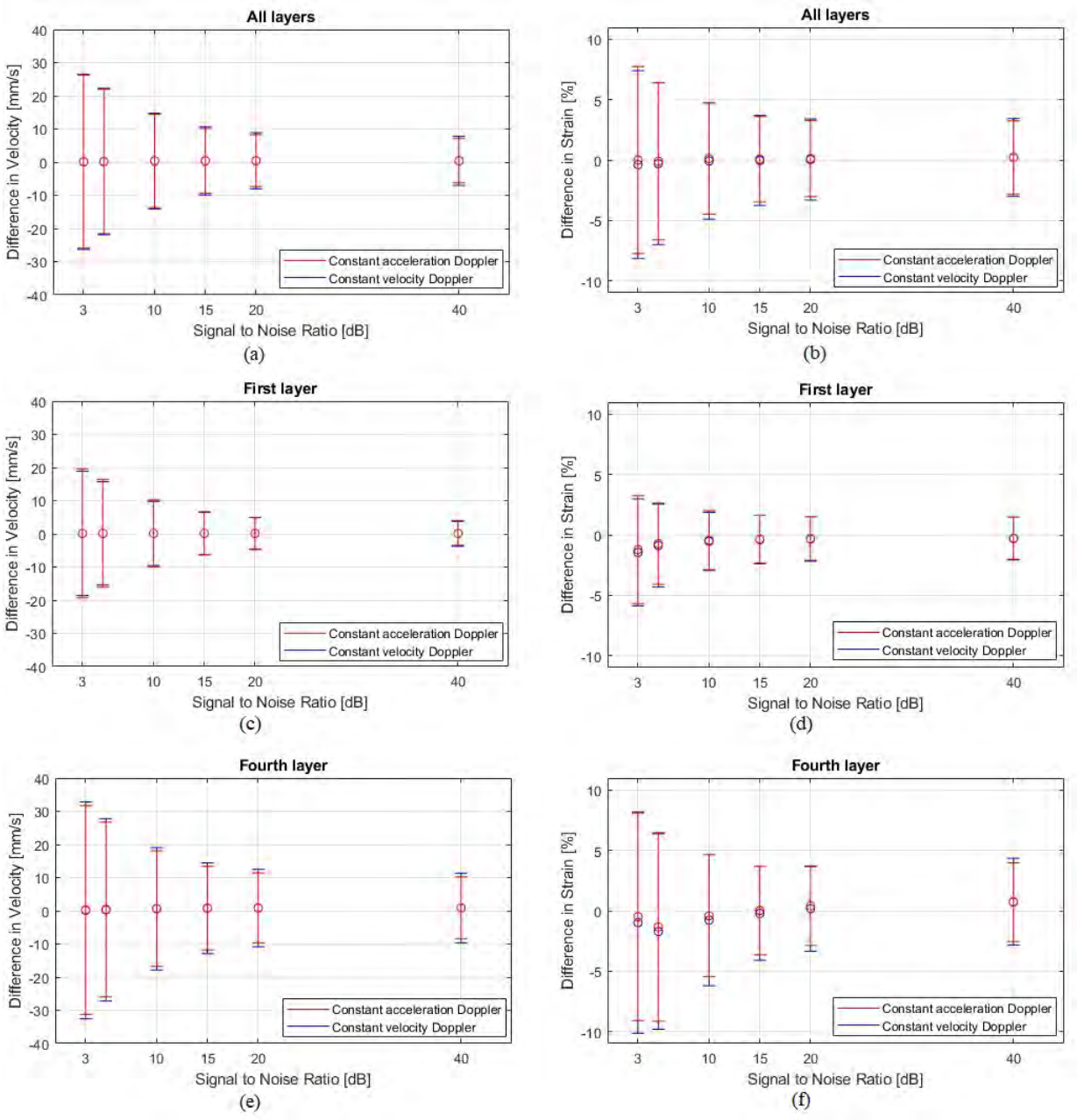

Figure 4.1: Comparison between the constant and constant acceleration Doppler estimators in the simulation model. Results are plotted as bias and SD for the difference between results from the estimators and the ground truth in the simulation model. Velocity estimates are shown in the left column, and strain estimates in the right column. Results from the constant velocity Doppler (blue) and constant acceleration Doppler (red) at all layers (a, b), at the first layer only (c, d), and at the fourth layer only (e, f). The myocardial layers are numbered from 1 to 4, starting at the epicardium.

method allows the velocity to vary within each Doppler pulse packet, and allows the constant acceleration Doppler to estimate velocity in greater detail than constant velocity

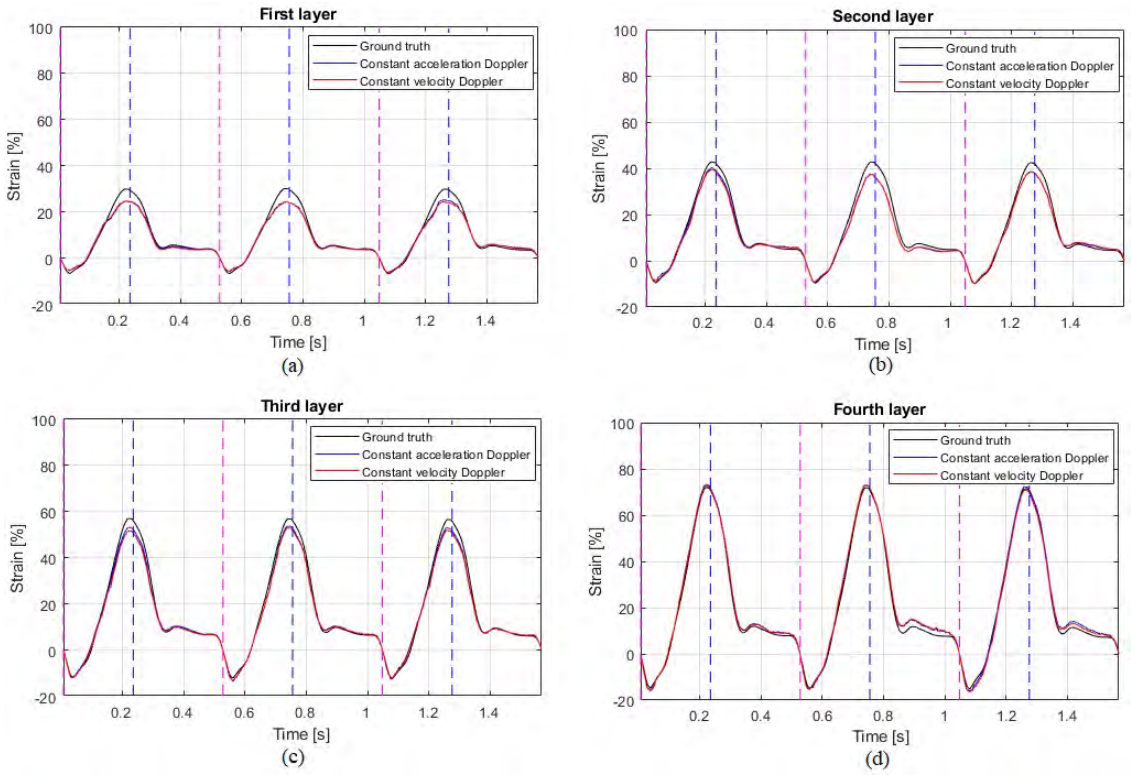

Figure 4.2: Estimated radial strain of four myocardial layers for data at 20 dB SNR from the first simulation in Table 2.3 by using constant velocity and constant acceleration Doppler methods. The myocardial layers are numbered from 1 to 4, starting at the epicardium. Strain in the first layer (sub-epicardial region) (a), second layer (b), third layer (c), and fourth layer (sub-endocardial region) (d). End-diastole is indicated with magenta and end-systole with blue vertical lines.

Doppler, especially for high velocities. This effect is more clearly observed in the fast motion region in Figures 4.1e, 4.1f, 4.2c and 4.2d, i.e. in the sub-endocardial region, while these two approaches give almost identical results in the slow motion region in Figures 4.1c, 4.1d, 4.2a and 4.2b, i.e. in the sub-epicardial and mid-myocardial regions. The results of the animal study agree with the simulation results, although the ground truth is not known for these results. The layer tracking from the two Doppler-based methods are almost identical in the sub-epicardium and mid-myocardium, but differ slightly in the sub-endocardium in Figure 4.3. Correspondingly, the difference in radial strains estimated from these two approaches is only observed in the deepest layer, the sub-endocardial region in Figure 4.4. For the simulated velocity, the variation with time is given by the nor-

malized derivative dk_1/dt of the compression factor $k_1(t)$, shown in Figure 2.5. As seen from the figure, dk_1/dt shows little variation in the intervals from 0.07 s to 0.13 s and from

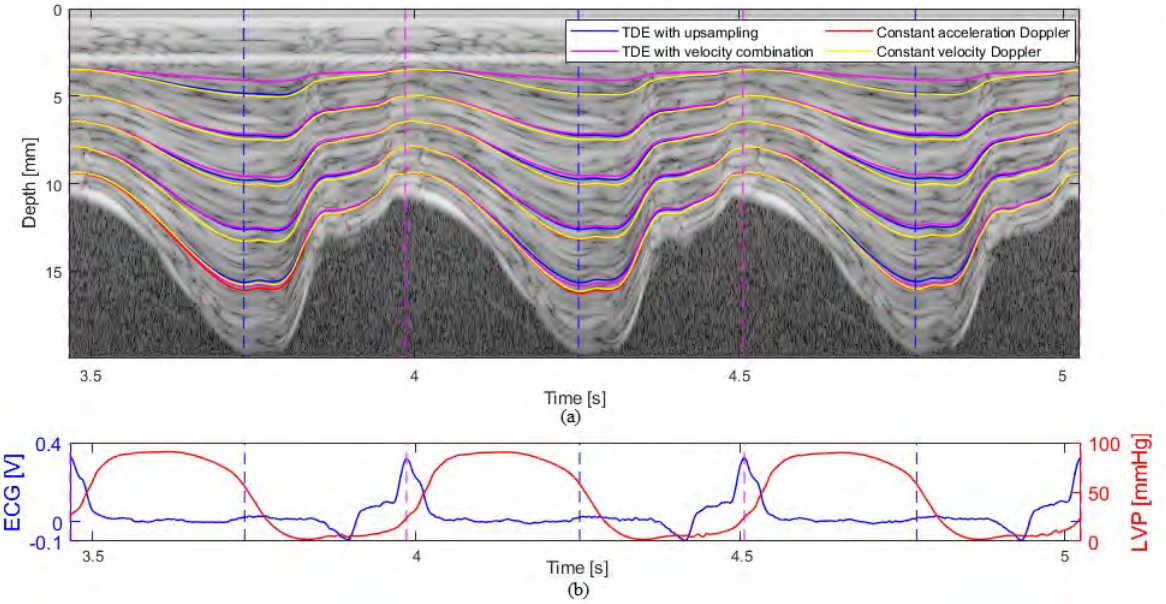

Figure 4.3: M-mode grey scale image with tracking of four myocardial layers, using data acquired from a representative animal. The myocardial layers are tracked using the TDE with upsampling (blue), the TDE with velocity combination (magenta), constant acceleration Doppler (red) and constant velocity Doppler (yellow) methods (a). Synchronously sampled ECG (blue) and left ventricular pressure (LVP) data (red) are shown below (b). End-diastole is indicated with magenta and end-systole with blue vertical lines.

0.3 s to 0.47 s, i.e. over 45% of the simulated cardiac cycle duration. The velocity estimates from the two Doppler methods are similar in these intervals, and a difference between these two methods is not clearly observed when the bias and STD are calculated over the whole simulated cardiac cycle. If tissue velocity varies linearly within a packet and a_1 in Eq.(2.21) is equal to e.g. 10% of a_0, the velocity estimated by constant velocity Doppler is $1.15a_0$. The velocity variation within the packet, in this example 15% of a_0, is neglected. If a_0 is equal to 70 mm/s, this corresponds to a velocity variation of 10 mm/s being overlooked. However, we could not see any clear effect due to velocity variations within each packet in our simulations, and neither in our few experimental data. Although we could not find a clear benefit of the constant acceleration Doppler method in our experiments, the method might still be beneficial in other applications involving larger acceleration. When the noise level is increased, the bias and variation in the strain estimates increase

almost similarly for the two methods Figure 4.1. Hence, the robustness to noise was not found to be different for the two Doppler-based estimators, and the constant acceleration Doppler is preferred by its ability to track faster motions.

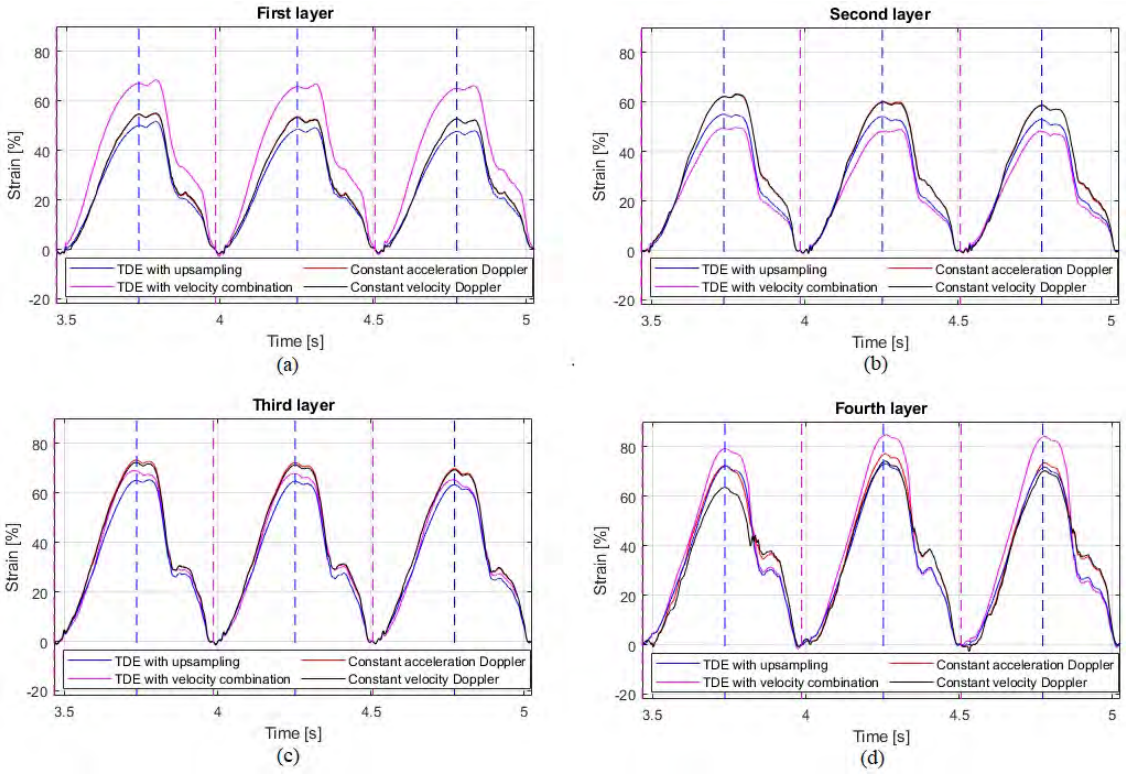

Figure 4.4: Estimated radial strain of four myocardial layers using data acquired from a representative animal, using the TDE with upsampling (blue), the TDE with velocity combination (magenta), the constant acceleration Doppler (red) and the constant velocity Doppler (black) methods. The myocardial layers are numbered from 1 to 4, starting at the epicardium. Strain in the first layer (sub-epicardial region) (a), second layer (b), third layer (c), and fourth layer (sub-endocardial region) (d). End-diastole is indicated with magenta and end-systole with blue vertical lines.

For the TDE methods, the myocardial layers from both methods seem to follow the motion of the myocardial tissue in the animal recordings Figure 4.3. This shows that limiting the maximum displacement between two RF lines to $\lambda/2$ was appropriate for this application. This also agrees with the results from the Doppler estimators, as this is also the limit for aliasing in a Doppler velocity calculation. TDE with upsampling was generally better, i.e. lower bias and SD, than TDE with velocity combination in both velocity and strain estimation at all SNR levels in Figure 4.5a and 4.5b. TDE with velocity combination showed its advantage over TDE with upsampling in the strain estimation in the slow motion region

for data with low noise levels, i.e. when the SNR was greater than or equal to 15 dB in Figure 4.5d. Even though a small improvement in velocity estimation was found when using TDE with velocity combination at all SNR levels in Figure 4.5c, TDE with upsampling had lower bias variation in strain estimation as SNR was lower than 15 dB (Figure 4.5d). At moderate noise level, SNR of 10 dB, the results from this estimator degraded in the sub-epicardial region. A reason for this may be that the TDE with velocity combination omits some scanlines to increase the velocity resolution. This makes the method more susceptible to noisy data sets, giving results that degrade faster than the TDE with upsampling for noisy data sets. This is even more evident for the highest noise levels, SNR of 3 and 5 dB, where spikes are seen in the velocity estimates. Signals with such spikes were interpreted as having a high maximum velocity, confusing the algorithm to use the V_1 estimate over the whole depth of the image. These phenomena can explain why the strain estimates from TDE with upsampling were better than those from TDE with velocity combination for noisy data sets, meaning SNR lower than 15 dB.This may explain why strain curve in the first layer calculated from TDE with velocity combination deviate markedly from those calculated from the other methods in Figure 4.4a. In the sub-endocardium, the fourth layer, TDE with upsampling was better than TDE with velocity combination in both and strain velocity estimation at all SNR levels, in Figure 4.5e and 4.5f. Although the ground truth is not known in these experimental investigations, the results strongly indicate that upsampling the scanlines prior to finding the cross-correlation enhanced the accuracy of the TDE method. A limitation of TDE with velocity combination is also shown in Figure 4.6d, in the end-diastolic region from 0.35 s to 0.45 s, where the myocardial tissue velocity at its minimum. In the sub-endocardial region, the estimator will optimize towards high maximum velocity, using the velocity estimate V_1, with a minimum detectable velocity before sub-sample interpolation of 48 mm/s. This reduces the accuracy in the time interval when the myocardium moves more slowly. This may explain why the strain curve from TDE with velocity combination in the fourth layer separates from the ground truth in this interval, while the strain curve calculated from TDE with upsampling was much better

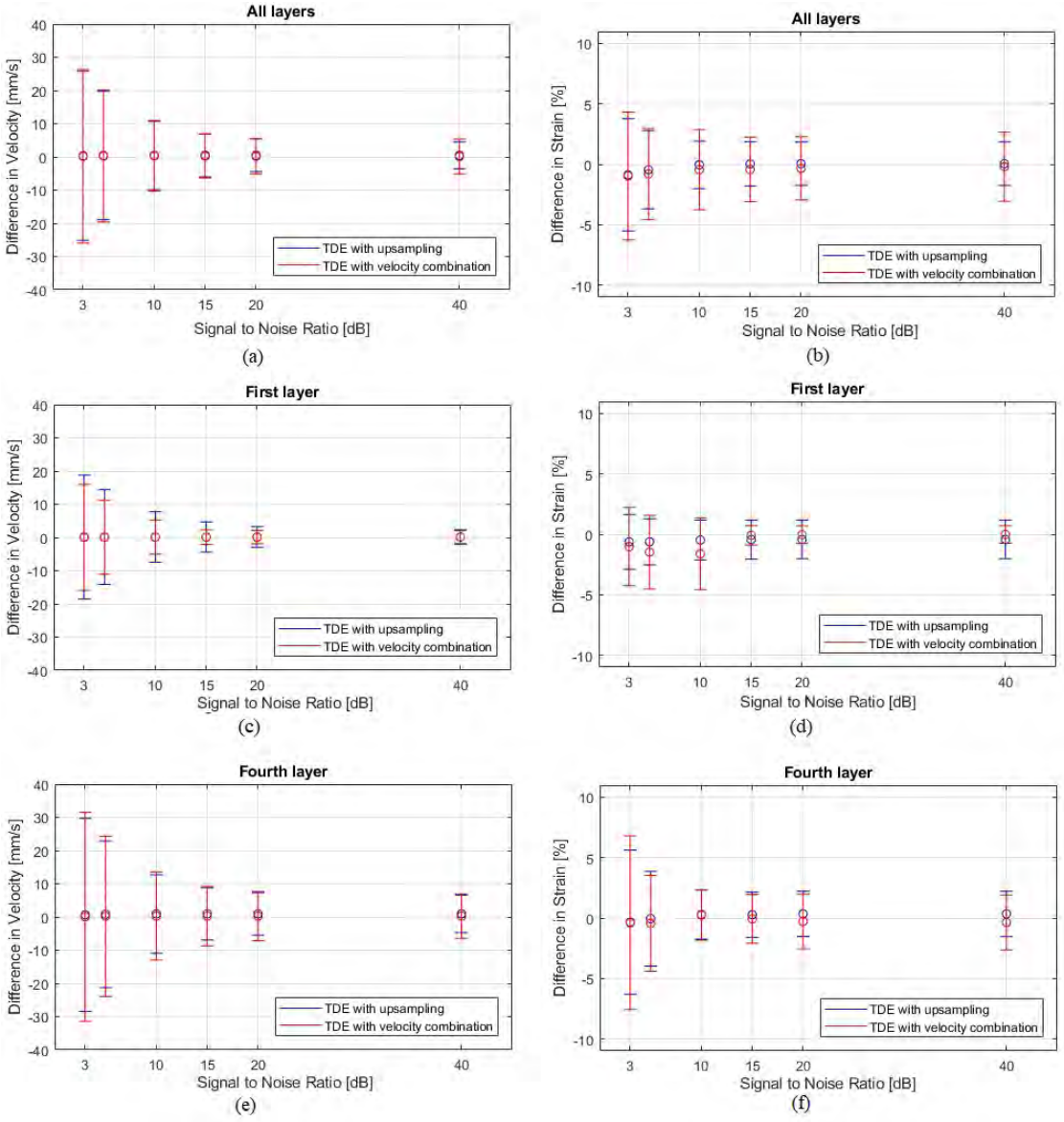

Figure 4.5: Comparison between two TDE-based estimators in the simulation model. Results are plotted as bias and SD for the difference between results from the estimators and the ground truth from the simulation model. Velocity estimates are shown in the left column, and strain estimates in the right column. Results from TDE with upsampling (blue) and TDE with velocity combination (red) at all layers (a, b); at the first layer only (c, d) (the most shallow layer); at the fourth layer only (e, f) (the deepest layer)

at following the ground truth. The end-systolic strains computed from TDE with upsampling, using the experimental data, increased monotonously from the sub-epicardial to the sub-endocardial region (Figure 4.4). However, the four myocardial layers mean there are only four data points in this curve, and this must be taken into account when interpreting this result. The computations were carried out in Matlab R2019b on a personal

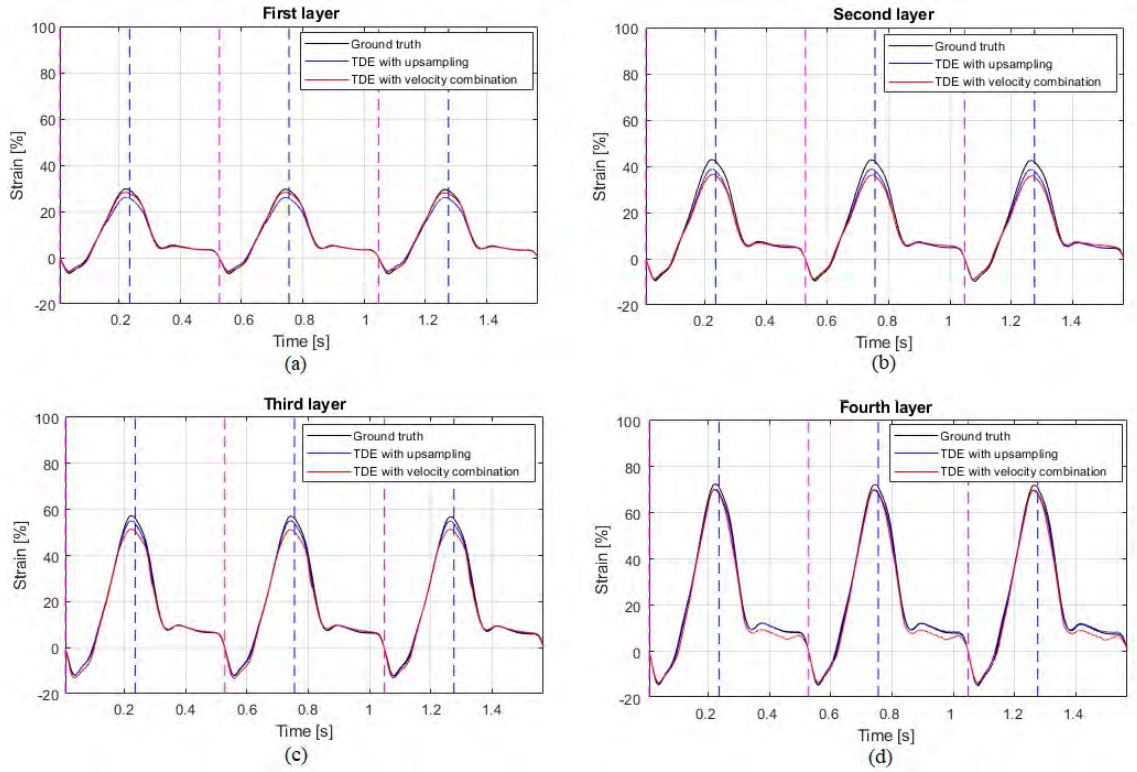

Figure 4.6: Estimated radial strain of four myocardial layers for data at 20 dB SNR from the first simulation in Table 2.3 by using TDE with upsampling and TDE with velocity combination methods. The myocardial layers are numbered from 1 to 4, starting at the epicardium. Strain in the first layer (sub-epicardial region) (a), second layer (b), third layer (c), and fourth layer (sub-endocardial region) (d). End-diastole is indicated with magenta and end-systole with blue vertical lines.

computer with an AMD Ryzen 1700 8-core processor running at 3 GHz, with 32 GB RAM. The calculation time needed to estimate velocity for all depths at one point in time, based on two recorded RF scanlines, was 4.4 ms for both Doppler methods, 108 ms for TDE with upsampling, and 10 ms for TDE with velocity combination. Hence, the TDE with upsampling and TDE with velocity combination required 25 times and 2.3 times longer calculation time than the Doppler methods, respectively. TDE with velocity combination was 11 times faster than TDE with upsampling. This calculation time can be compared to the pulse repetition interval T_{prf}, which was 0.4 ms in this study. Hence, real-time operation on this system with the present settings would require approximately 10 times faster processing for the Doppler methods, 25 times faster for TDE with velocity combination, and 270 times faster for the TDE with upsampling. Estimation of the center frequency (Paper B) consumed a large part of the calculation time for the Doppler methods. If this is

omitted, the calculation times for the Doppler methods was 1.4 ms. However, this would degrade the accuracy of the estimates.

The velocity of myocardial tissue from the simulation model increased with depth. In this application, we can only see between two Doppler methods in the deep region. The computation times for the two Doppler-based methods was equal, but constant acceleration Doppler gave slightly better results in the fast motion region, making this the preferred of the Doppler-methods. The TDE-based methods were found to give better results than the constant acceleration Doppler, both for velocity and strain (Figures 4.1a, 4.1b, 4.5a, and 4.5b). The quality of the results from the constant acceleration Doppler degraded more rapidly than those from the TDE-based methods as the signal quality was decreased, indicating that the TDE methods are more robust against noise than the constant acceleration Doppler. The echo strength decreases with depth; hence, the accuracy of the estimates degrades with increasing depth, and more for the constant acceleration Doppler method. Moreover, TDE with velocity combination showed its advantage over constant acceleration Doppler in the radial strains Figures 4.1 and 4.5. One source of error for the TDE method was the limited velocity and spatial resolutions, the latter linked to the kernel size. The spatial velocity resolution from the phase Doppler estimators is 39 μm while that from TDE methods is 308 μm. The results of the myocardial layer tracking using constant acceleration Doppler and TDE with upsampling were found to separate gradually as the depth increased in Figure 4.3. Both Doppler methods assume that the velocities within one pulse packet vary as a monotonic function with time. This assumption can limit the ability to capture quick and short phase changes in the myocardial motion, see e.g. around 3.9 s in Figure 4.4. This may explain why the strains calculated from the two Doppler methods were different from those from the TDE methods during the short contraction phase. The strain curves of the four myocardial layers found from TDE with upsampling (Figure 4.6) were almost similar between the heart cycles, while those from constant acceleration Doppler varied more between the heart cycles. This indicates that the TDE was more robust than the constant acceleration Doppler, but since the ground truth was unknown for the animal model recordings, it cannot be ruled out that this was a real variation.

The data were acquired using transducers attached directly to the heart surface. This solution minimized the problem of insonification angle, and the reduced depth allowed a high PRF, which is beneficial for velocity estimates. The results showed the TDE with upsampling method gave slightly lower variation than the constant acceleration Doppler when compared to simulation results. The accuracy of Doppler-based methods has been reported to be more susceptible to noise than that from the TDE method [24, 26], and our results confirm this. The results from TDE with velocity combination lie somewhere between constant acceleration Doppler and TDE with upsampling when looking at accuracy, robustness and computation time. A pilot study using this recording system has showed that a minor blood flow reduction in the left anterior descending coronary artery (LAD) resulted in decreased radial strain in the sub-epicardium [39]. In such applications, TDE with velocity combination can be employed to detect small changes in radial strain in the sub-epicardial region. However, this requires low noise in the acquired data, i.e. SNR better than 15 dB. The robustness of TDE with velocity combination can be improved by using fewer velocity components, e.g. using only the V_1 and V_2 estimates. This also reduces processing time but degrades the velocity resolution in the shallow regions. TDE with upsampling is very computer-intensive, which may be challenging in a real-time system. The choice of velocity estimation method will be a balance between the fast Doppler methods, the computationally heavy but more robust TDE with upsampling, with an intermediate solution being the moderately robust, accurate and time-consuming TDE with velocity combination. The constant acceleration Doppler method might be the best choice for a light real-time processing system, while TDE with upsampling may be preferred for studies of the finer details of myocardial deformation if real-time operation is not essential.

The endocardial boundary detection was based on Fuzzy logic supported by a combination of a maximum filter, removal of outliers, and snake regularization. The result indicates that this procedure was able to track the endocardial border as shown in Figure 4.7. Some further improvement could be achieved by in addition requiring monotonous expansion during systole (red line in Figure 4.7), but this difference is not dramatic. The apparent improvement achieved by this requirement must be weighed against the risk of imposing too strict restrictions to the myocardial motion. This border detection method

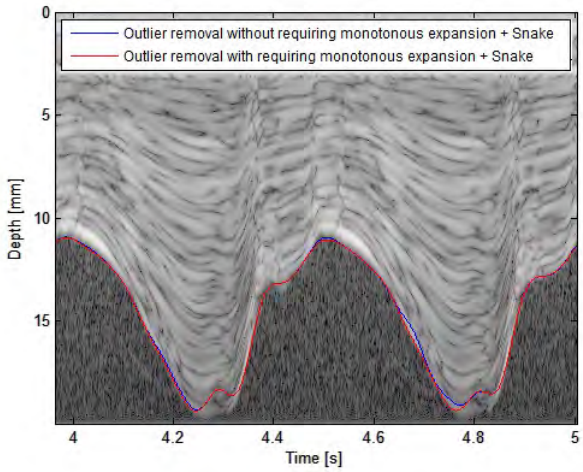

Figure 4.7: Gray scale M-mode image with the detected endocardial border with no requirements (blue), and requiring monotonous expansion during systole (red)

does not work well when the border is too close to the edge of the image, as the method organizes pixels in a 3x3 mask. The precision is possibly improved by doing alignment for detected epicardial border in several cycles. However, it is imposed to the risk of abnormality detection. The border could also outlined by the cardiologist to attain more accurate result for noisy data or to overcome limits of the boundary detection method.

4.1 Clinical Applications

4.1.1 Radial strain distribution across cardiac wall

Different radial strain distributions have been reported [4, 14–16]. A preliminary study about transmural strain distribution was carried on five recordings from one pig using the ultrasound system. The myocardium was divided into 5 equally sized layers. Tissue velocities (V) were estimated from the acquired RF signals using the sum of absolute differences after up-sampling the RF. The initial V estimates were regularized by fitting an active contour through the TDE's results versus depth. Clear differences in the end-systolic radial strain distribution were observed between apical and basal segments of the heart as shown in Figure 4.8. The radial strain increased from the epi- to endocardium in the apical segment while the highest strain values were observed more towards the mid-myocardium

near the base. These findings are in agreement with finite element model (FEM) results [16] suggesting that differences in transmural strain distribution could be due to differences in curvature at the base and apex.

The study was extended by fitting second order polynomials to the end-systolic strain value, obtained after normalization of the myocardial thickness. The myocardial wall was also divided into 5 equally sized layers. However, signal processing method was modified. Tissue velocities were estimated as a function of depth using phase shift Doppler. A fourth order Butterworth filters were applied to reduce noise in the velocity estimates, in both depth and time directions. The results were averaged over all acquisitions at each measurement site. The initial results from four experimental data in Figure 4.9 show a concave transmural strain profile near the apex, and a convex strain profile near the base of the left ventricle. Near the apex, the maximal radial strain occurred at the endocardial border, while near the base, the highest strains were found more towards the mid-myocardium.

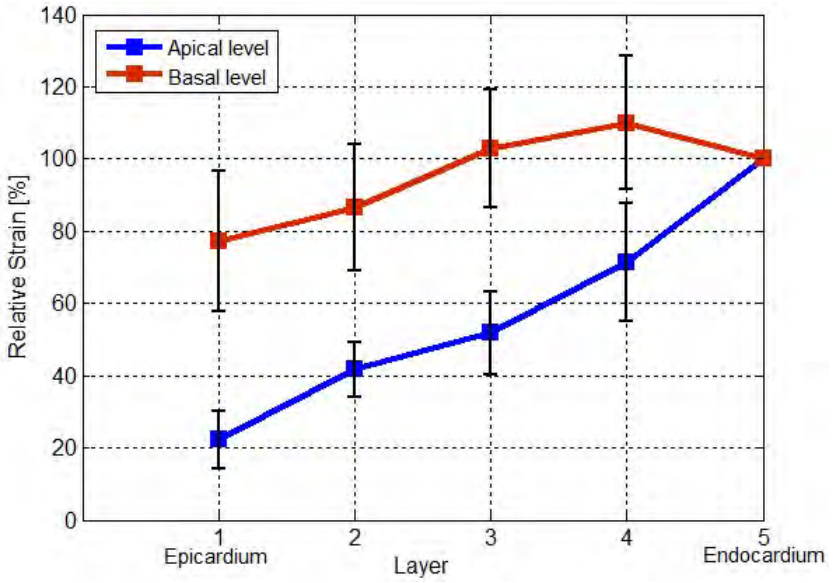

Figure 4.8: Radial strain distribution at the apex and the base in five layers at end-systole relative to endocardial layer. Bars show the SD of the 5 recordings.

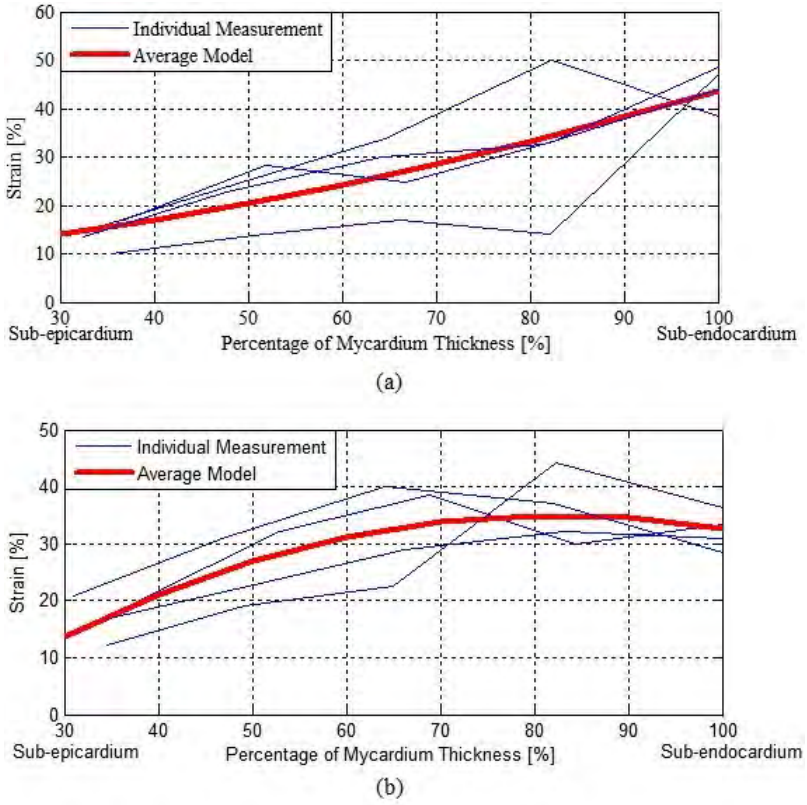

Figure 4.9: Strain profile estimated through the myocardium. Individual measurements and average model for strain profile. (a) – At the apex, (b) – At the base.

4.1.2 Effect of myocardial perfusion on end-systolic radial strain at the apex

According to the literature, subendocardial strain is more susceptible to reduced perfusion than mid-myocardial and sub-epicardial strains. A pilot study on four pigs was carried out to observe the change in behavior of different myocardial layers under various flow conditions. The blood flow in the left anterior descending coronary artery (LAD) was controlled under three flow conditions: no flow reduction, 25% flow reduction and 75% flow reduction. The myocardium wall was divided into three equally sized layers. Tissue velocities were estimated from the RF signals using a phase shift Doppler estimator, finding the average phase shift between four successive RF lines. A fourth order Butterworth filter was applied to the velocity estimates in both temporal and spatial directions, and radial strain rate and strain were calculated. We noticed the different reaction of different myocardial layers under a graded flow reduction at end-systole in Figure 4.10. At 25% flow reduction,

the strain reduction was larger in the sub-endocardial than the mid- and sub-epicardial layers. At 75% flow reduction, the strain reduction was more similar in the different layers. The strain decreased by 16.4±7.2% in the sub-endocardium, while it decreased by 7.9±4.9% and 7.7±6.8%, respectively, in the mid- and sub-epicardial layers at 25% flow reduction. At 75% flow reduction, the strain was reduced by 28.1±7.7% compared to baseline in the sub-endocardial and mid-layers, while it was reduced by a similar amount in the mid-myocardium and sub-epicardium, 26.9±6.5% and 26.8±10.7%, respectively.

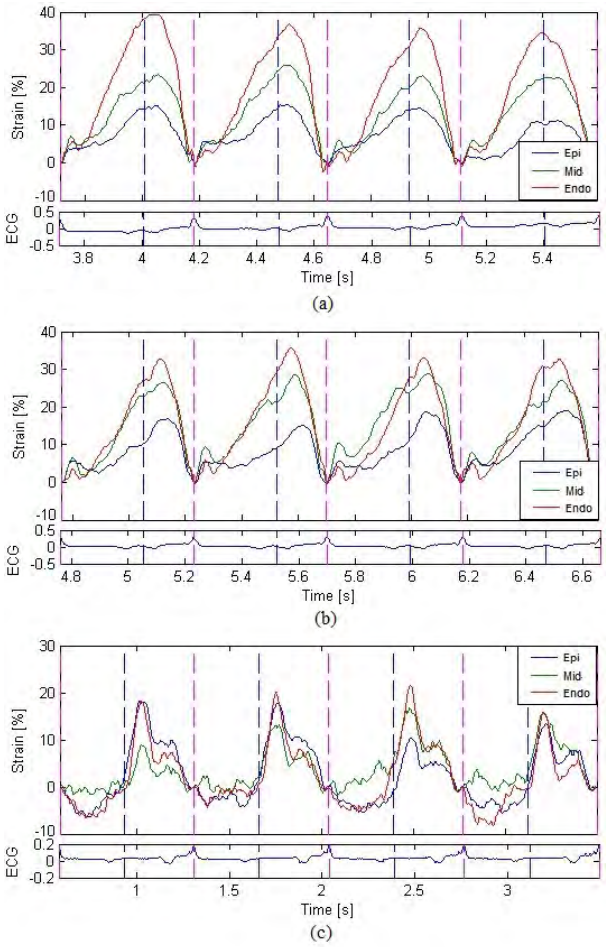

Figure 4.10: Estimated radial strain of three myocardial layers under different flow conditions. (a) – No flow reduction, (b) – 25% flow reduction, (c) – 75% flow reduction

The long-term goal of this study is to develop a monitoring tool for patients during and after cardiac surgery, but it can also be useful as a research tool for fundamental studies, offering detailed information on heart mechanics. Some initial results were observed by using the measurement system together with the suitable signal processing method. Note

the main goal of this thesis was to develop and investigate the technology, i.e. the signal processing and algorithms, and the clinical results are examples of what type of results can be obtained from the system. No clinical conclusion should be drawn from this thesis.

4.2 Conclusion

The results of this work can be summarized as follows:

- The measurement system using miniature ultrasound transducers was demonstrated to be able to provide depth-dependent information about myocardial motion, such as velocity and strain.
- The conventional Doppler and time delay estimators were modified to better handle the variation of tissue velocity along the depth. The evaluation of these velocity estimation methods were carried out using data from both the simulation model and experiment. All estimators could be used to estimate tissue velocity in most situations, but there was difference in quality and processing time.
- The data processing methods and myocardium simulation model were implemented in Matlab, to make the method available for other researchers. This data processing package with a graphical user interface can support clinicians in analyzing and interpreting data.
- Initial results of cardiac mechanics were obtained from the experimental data. These are transmural strain profiles as a function of myocardial depth at different sites of the left ventricle, and effect of myocardial perfusion on the end-systolic radial strain at the apex.

Chapter 5

Summary of Contributions

This section presents the summary of contributions included in this thesis. The thesis contains one paper published in a peer-reviewed journal *Paper A*, one paper submitted to a peer-reviewed journal *Paper B*, three papers published as proceedings from international conferences *Paper C, Paper D, Paper E*, and one unpublished paper written as a technical manual *Paper F*. These papers presents the entire PhD work.

List of Papers Included in this Thesis

Papers in international peer-reviewed journals

1. **Thuy Thu Nguyen**, Andreas W. Espinoza, Stefan Hyler, Espen W. Remme, Jan D'hooge, and Lars Hoff, "Estimating Regional Myocardial Contraction Using Miniature Transducers on the Epicardium,"

Papers submitted to international peer-reviewed journals

1. **Thuy Thu Nguyen**, Andreas W. Espinoza, Stefan Hyler, Espen W. Remme, Jan D'hooge, and Lars Hoff, "Myocardial strain measured by epicardial transducers – comparison between velocity estimators" manuscript submitted to *Ultrasound in Medicine and Biology*.

Published proceedings from international conferences

1. **Thuy Thu Nguyen**, Andreas W. Espinoza, Espen W. Remme, Jan D'hooge, and Lars Hoff, "Transmural Myocardial Strain Distribution Measured at High Spatial and Temporal Resolution," in *Proc. IEEE Ultrasonics Symposium*, 2011.

2. **Thuy Thu Nguyen**, Andreas W. Espinoza, Stefan Hyler, Espen W. Remme, Jan D'hooge, and Lars Hoff, "Effect of Myocardial Perfusion on End-systolic Radial Strain at the Apex," in *Proc. IEEE Ultrasonics Symposium*, 2012.

3. **Thuy Thu Nguyen**, Andreas W. Espinoza, Stefan Hyler, Espen W. Remme, Jan D'hooge, and Lars Hoff, "Transmural Strain Distribution across the Cardiac Wall and Its Dependency on Measurement site," in *Proc. IEEE Ultrasonics Symposium*, 2012.

4. **Thuy Thu Nguyen**, Andreas W. Espinoza, Stefan Hyler, Espen W. Remme, Jan D'hooge, and Lars Hoff, "Velocity Resolution Improvement for High Temporal Resolution Ultrasonic Transducer," in *Proc. IEEE Ultrasonics Symposium*, 2017.

Related presentations and posters not included in the thesis

Presentations at International Conferences

1. **Thuy Thu Nguyen**, Andreas W. Espinoza, Espen W. Remme, Jan D'hooge, and Lars Hoff, "Transmural Myocardial Strain Distribution Measured at High Spatial and Temporal Resolution," in *Proc. IEEE Ultrasonics Symposium*, 2011.

2. **Thuy Thu Nguyen**, Andreas W. Espinoza, Stefan Hyler, Espen W. Remme, Jan D'hooge, and Lars Hoff, "Effect of Myocardial Perfusion on End-systolic Radial Strain at the Apex," in *Proc. IEEE Ultrasonics Symposium*, 2012.

3. **Thuy Thu Nguyen**, Andreas W. Espinoza, Stefan Hyler, Espen W. Remme, Jan D'hooge, and Lars Hoff, "Transmural Strain Distribution across the Cardiac Wall and Its Dependency on Measurement site," in *Proc. IEEE Ultrasonics Symposium*, 2012.

4. **Thuy Thu Nguyen**, Andreas W. Espinoza, Stefan Hyler, Espen W. Remme, Jan D'hooge, and Lars Hoff, "Velocity Resolution Improvement for High Temporal Resolution Ultrasonic Transducer," in *Proc. IEEE Ultrasonics Symposium*, 2017.

Presentations at National Conferences

1. **Thuy Thu Nguyen**, and Lars Hoff, "A New Method to Measure Myocardial Strain Distribution at High Spatial and Temporal Resolution," presentation at *35th Scandinavian Symposium on Physical Acoustics*, Geilo, Norway, 29 January - 1 February 2012.

5.1 Summary of Papers Included in the Thesis

Paper A: Estimating Myocardial Contraction Using Miniature Transducer on the Epicardium

This paper describes the hardware implementation of the measurement system and proves feasibility of this system in getting information about the motion of myocardium. The system was tested on a porcine model. Two 3 mm diameter, 10 MHz ultrasound transducers were mounted on the heart's surface in order to monitor regional heart motion continuously.

The endocardial border was detected using an algorithm based on fuzzy logic with filtering to reduce noise and remove outliers, and the myocardium was divided into 4 equally sized layers at end-diastole. The radial tissue velocity was estimated by using time delay estimates based on cross-correlation between successive RF scanlines. The velocity estimates were then employed to estimate radial strain rate and strain, and to track the motion of myocardial layers.

The results showed that the measurement system together with the signal processing algorithm could be used to track myocardial deformation and study regional radial strain. The high temporal resolution allowed detecting changes in phases during the myocardial motion. The high spatial resolution in combination with up-sampling and TDE increased

the accuracy of the velocity estimates.

The hardware implementation of the measurement system was realized by professor Lars Hoff, and the animal experiments were carried out by dr. med. Andreas W. Espinoza. Development of the signal processing algorithms, software code implementation, testing and adapting the methods to the experimental data, and all result analysis was done by candidate.

This paper was published Ultrasound in Medicine and Biology, 2019 [40].

Paper B: Myocardial strain measured by epicardial transducers – comparison between velocity estimators

The paper presents a modification for the TDE method to satisfy different requirements at different myocardial regions and an extension to the phase shift Doppler estimator to increase the accuracy of the velocity estimates. A simulation model was developed to compare the performance of the estimators towards known results. This model simulates ultrasound echoes from the moving myocardium, based on published models for myocardial motion patterns and using the ultrasound simulation tool Field II. Results from the velocity estimators were tested against the simulation model and on ultrasound recordings from five animals.

The velocity varies through the contracting myocardium relative to the epicardial surface, and the conventional Doppler and TDE algorithms were modified to compensate for this variation. The modified Doppler algorithm allows the velocity to vary linearly within the pulse packet. This was denoted constant acceleration Doppler. The TDE methods were modified by either upsampling the received radio-frequency (RF) scanlines by a factor 10 prior to applying the cross-correlation, or processing the RF lines differently depending on depth into the myocardium. The latter was done by correlating every 2^{nd}, 3^{rd} or 4^{th} scanline in the slow-moving sub-epicardial regions, while correlating all scanlines in the faster moving sub-endocardial region. The latter method was made adaptive, using the results to determine how many scanlines to skip at some depth. Radial strain rate was calculated by first segmenting the myocardium into 4 layers of equal thickness. The strain rate was then estimated from the velocity variation within each layer by linear regression,

using the velocity estimates as input. Strain was estimated by temporal integration of the strain rate, adding global drift-compensation. A Bland-Altman test comparing the results from the methods to the ground truth from the simulation model were performed.
It was found that the constant acceleration Doppler method performed better than conventional phase shift Doppler in capturing details in the sub-endocardium, where the highest velocities are found. No difference between the Doppler methods was found closer to the epicardium. TDE with upsampling performed well in all situations, showing low bias and variance in velocity and strain estimates at all noise levels and in both slow and fast moving regions. TDE using a velocity combination to process results differently in slow and fast moving regions showed intermediate performance, with accuracy and robustness between TDE with upsampling and constant acceleration Doppler.Large differences in computing time was found between the different estimation methods. TDE with upsampling required 25 times more computing time than the Doppler methods, while TDE with velocity combination required 2.3 times more time. Estimation of the centre frequency consumed a large part of the computing time for the Doppler methods, omitting this reduced the computing time further by a factor 3. The best performance was achieved by synthetically upsampling the RF scanlines prior to applying the time-delay estimator. The long computing time required by this method may make it most suited in a laboratory setting where real-time operation is not necessary, while the faster constant acceleration Doppler may be preferred in a light real-time system.
The animal experiment and RF signals recording were done by dr. med. Andreas W. Espinoza. The data for Waks model [37, 38] and the script for re-calculating the scatterers positions based on the motion of the meshing nodes in the simulation were given by professor Jan D'hooge. Development of the signal processing algorithms, implementation of the simulation model and signal processing algorithms in Matlab, testing of the algorithms on the simulated and experimental data, and all result analysis and comparison was done by candidate.

This paper is was submitted to Ultrasound in Medicine and Biology soon. This is an extended version of a paper pusblished in the IEEE International Ultrasonics Syposium Proceedings 2017 [32].

Paper C: Transmural Myocardial Strain Distribution Measured at High Spatial and Temporal Resolution

The paper investigates differences in transmural myocardial strain distribution at two different regions in the left ventricle: one at the apex, one at the base. The analysis was carried out on five recordings from one animal, done during baseline conditions between cardiovascular interventions. Tissue velocities (V) were estimated from the acquired RF signals using a time-delay estimator (TDE) after up-sampling the RF traces. The initial V estimates were regularized by fitting an active contour through the TDE's results versus depth.

The results showed that radial strain increased through the myocardium, from the epi- to endocardium, in recordings from the apical segment. On the recordings taken near the base, the highest strain values were observed more towards the mid-myocardium. These findings are in agreement with finite element model (FEM) results suggesting that differences in transmural strain distribution could be due to differences in local curvature at the base and apex. However, this preliminary result served mainly as an indication of the potential of the ultrasound measurement system and the signal processing methods, and no general physiological conclusion should be drawn from this.

The hardware implementation of the measurement system was realized by professor Lars Hoff, and the animal experiments were carried out by dr. Andreas W. Espinoza. The signal processing development, software code implementation, applying the method to the experimental data, and analyzing and interpreting the results was done by candidate.

This paper has been pusblished in the IEEE International Ultrasonics Syposium Proceedings 2011, pp. 696-699 [22].

Paper D: Transmural Strain Distribution across the Cardiac Wall and Its Dependency on Measurement Site

The transmural behavior of myocardial deformation remains a matter of debate, with conflicting findings in literature. The aim of this study was to use our system to measure the transmural strain profiles at different sites inside myocardium of the left ventricle, using

two transducers: one in the apical region, one near the basal region. The data analysis was done on four recordings from one animal. The myocardial wall was divided into 5 equally sized layers at end-diastole. Tissue velocities were estimated as a function of depth using phase shift Doppler. Second order polynomials were fit to the end-systolic strain values, obtained after normalization of the myocardial thickness. The results were averaged over all acquisitions at each measurement site. The results show a concave transmural strain profile near the apex, and a convex strain profile near the base of the left ventricle. Near the apex, the maximal radial strain occurred at the endocardial border, while near the base, the highest strains were found more towards the mid-myocardium.

The hardware implementation of the measurement system was realized by professor Lars Hoff, and the animal experiments were carried out by dr. Andreas W. Espinoza. The signal processing algorithm development, software code implementation, applying the method to the experimental data, and analyzing and interpreting the results was done by candidate.

This paper has been pusblished in the IEEE International Ultrasonics Syposium Proceedings 2012, pp. 1-4 [41].

Paper E: Effect of Myocardial Perfusion on End-systolic Radial Strain at the Apex

This paper compares radial strain in three myocardial layers under various levels of flow reduction, using two miniature transducers sutured to the epicardial surface: one at the apex, near the intervention area, and one near the base, far from intervention area. The blood flow in the left anterior descending coronary artery (LAD) was controlled under three flow conditions: no flow reduction, 25% flow reduction and 75% flow reduction. The recordings were made 15 minutes after the intervention. The experiments were carried out on four pigs.

Tissue velocities were estimated from the RF signals using a phase shift Doppler estimator. A 4^{th} order Butterworth filter was applied to the velocity estimates in both temporal and spatial directions. The myocardial wall was divided into three equally sized layers.

The results showed differences in the how different myocardial layers react on a graded flow reduction. At 25% flow reduction, the strain reduction was larger in the sub-endocardial

than the mid- and sub-epicardial layers. At 75% flow reduction, the strain reduction was more similar in the different layers. Although no clinical conclusion can be drawn from such a limited experiment, the results indicate the potential of our measurement system to provide novel insight into cardiac mechanics, e.g. the response of different myocardial layers to a reduced blood flow.

The hardware implementation of the measurement system has been realized by Professor Lars Hoff, and the animal experiments were carried out by dr. med. Stefan Hyler. The signal processing algorithm development, software code implementation, applying the method to the experimental data, and analyzing and interpreting the results was done by candidate.

This paper has been pusblished in the IEEE International Ultrasonics Syposium Proceedings 2012, pp. 1-4 [39].

Paper F: Implementation and Use of the Software. Data Processing Algorithms and Simulation of Myocardial Motion

This paper gives a more detailed description of the software developed in the project than what is possible in a published scientific paper, and it also serves as a user manual for how to run the software. The intention is to make the methods available for other researchers, including both clinicians applying the methods to new data, and technologists developing the methods further.

The paper describes the implementation of the signal processing algorithms, the data processing procedure and the myocardium simulation model in Matlab. User friendly graphical interfaces are provided for both data analysis and running the simulation model. The data analysis interface shows the results of velocity estimates (from TDE or Doppler methods), myocardial layers, strain rate and strain. Both translation and rotation motions of the insonified myocardium were supported in the simulation.

The script for re-calculating scatterer position from the motion of the meshing nodes was provided by professor Jan D'hooge. Everything else was done by the candidate, including both algorithm development and implementation of algorithms and user interfaces.

This paper has been prepared as a report for internal use.

Bibliography

[1] H. M. Hurlburt, G. P. Aurigemma, J. C. Hill, A. Narayanan, W. H. Gaasch, C. S. Vinch, T. E. Meyer, and D. A. Tighe, "Direct ultrasound measurement of longitudinal, circumferential, and radial strain using 2-dimensional strain imaging in normal adults", *Echocardiography*, vol. 24, no. 7, pp. 723–731, 2007.

[2] N. Risum, S. Ali, N. T. Olsen, C. Jons, M. G. Khouri, T. K. Lauridsen, Z. Samad, E. J. Velazquez, P. Sogaard, and J. Kisslo, "Variability of global left ventricular deformation analysis using vendor dependent and independent two-dimensional speckle-tracking software in adults", *Journal of the American Society of Echocardiography*, vol. 25, no. 11, pp. 1195–1203, 2012.

[3] S. Langeland, P. F. Wouters, P. Claus, H. A. Leather, B. Bijnens, G. R. Sutherland, F. E. Rademakers, and J. D'hooge, "Experimental assessment of a new research tool for the estimation of two-dimensional myocardial strain", *Ultrasound in medicine & biology*, vol. 32, no. 10, pp. 1509–1513, 2006.

[4] K. Matre, T. Fanneløp, G. O. Dahle, A. Heimdal, and K. Grong, "Radial strain gradient across the normal myocardial wall in open-chest pigs measured with doppler strain rate imaging", *J Am Soc Echocardiogr*, vol. 18, no. 10, pp. 1066–1073, Oct. 2005.

[5] K. Matre, C. A. Moen, T. Fanneløp, G. O. Dahle, and K. Grong, "Multilayer radial systolic strain can identify subendocardial ischemia: An experimental tissue doppler imaging study of the porcine left ventricular wall", *Eur J Echocardiogr*, vol. 8, no. 6, pp. 420–430, Dec. 2007.

[6] R. M. Ellis, D. L. Franklin, and R. F. Rushmer, "Left ventricular dimensions recorded by sonocardiometry", *Circ. Res.*, vol. 4, no. 6, pp. 684–688, Nov. 1956.

[7] B. Bugge-Asperheim, S. Leraand, and F. Kiil, "Local dimensional changes of the myocardium measured by ultrasonic technique", *Scand. J. Clin. Lab. Invest.*, vol. 24, no. 4, pp. 361–371, Dec. 1969.

[8] C. J. Hartley, L. A. Latson, L. H. Michael, C. L. Seidel, R. M. Lewis, and M. L. Entman, "Doppler measurement of myocardial thickening with a single epicardial transducer", *Am. J. Physiol.*, vol. 245, no. 6, H1066–1072, Dec. 1983.

[9] F. Weidemann, B. Eyskens, F. Jamal, L. Mertens, M. Kowalski, J. D'Hooge, B. Bijnens, M. Gewillig, F. Rademakers, L. Hatle, and G. R. Sutherland, "Quantification of regional left and right ventricular radial and longitudinal function in healthy children using ultrasound-based strain rate and strain imaging", *J Am Soc Echocardiogr*, vol. 15, no. 1, pp. 20–28, Jan. 2002.

[10] M. Kowalski, T. Kukulski, F. Jamal, J. D'hooge, F. Weidemann, F. Rademakers, B. Bijnens, L. Hatle, and G. R. Sutherland, "Can natural strain and strain rate quantify regional myocardial deformation? a study in healthy subjects", *Ultrasound Med Biol*, vol. 27, no. 8, pp. 1087–1097, Aug. 2001.

[11] J. D'hooge, A. Heimdal, F. Jamal, T. Kukulski, B. Bijnens, F. Rademakers, L. Hatle, P. Suetens, and G. R. Sutherland, "Regional strain and strain rate measurements by cardiac ultrasound: Principles, implementation and limitations", *Eur J Echocardiogr*, vol. 1, no. 3, pp. 154–170, Sep. 2000.

[12] T. Kukulski, F. Jamal, J. D'Hooge, B. Bijnens, I. De Scheerder, and G. R. Sutherland, "Acute changes in systolic and diastolic events during clinical coronary angioplasty: A comparison of regional velocity, strain rate, and strain measurement", *J Am Soc Echocardiogr*, vol. 15, no. 1, pp. 1–12, Jan. 2002.

[13] T. Kukulski, F. Jamal, L. Herbots, J. D'hooge, B. Bijnens, L. Hatle, I. De Scheerder, and G. R. Sutherland, "Identification of acutely ischemic myocardium using ultrasonic strain measurements. a clinical study in patients undergoing coronary angioplasty", *J. Am. Coll. Cardiol.*, vol. 41, no. 5, pp. 810–819, Mar. 5, 2003.

[14] J. D'hooge, J. Schlegel, P. Claus, B. Bijnens, J. Thoen, F. V. d. Werf, G. R. Sutherland, and P. Suetens, "Evaluation of transmural myocardial deformation and reflectivity

characteristics", in *2001 IEEE Ultrasonics Symposium. Proceedings. An International Symposium (Cat. No.01CH37263)*, vol. 2, 2001, 1185–1188 vol.2.

[15] H. F. Choi, J. D'hooge, F. E. Rademakers, and P. Claus, "Distribution of active fiber stress at the beginning of ejection depends on left-ventricular shape", *Conf Proc IEEE Eng Med Biol Soc*, vol. 2010, pp. 2638–2641, 2010.

[16] H. F. Choi, F. E. Rademakers, and P. Claus, "Left-ventricular shape determines intramyocardial mechanical heterogeneity", *Am. J. Physiol. Heart Circ. Physiol.*, vol. 301, no. 6, H2351–2361, Dec. 2011.

[17] H. Skulstad, S. Urheim, T. Edvardsen, K. Andersen, E. Lyseggen, T. Vartdal, H. Ihlen, and O. A. Smiseth, "Grading of myocardial dysfunction by tissue doppler echocardiography: A comparison between velocity, displacement, and strain imaging in acute ischemia", *J. Am. Coll. Cardiol.*, vol. 47, no. 8, pp. 1672–1682, Apr. 18, 2006.

[18] "Source: Global health estimates 2016: Death by cause, age, sex, by country and by region, 2000–2016. geneva", *World Health Organization*, 2018.

[19] L. Hoff, A. Espinoza, and H. Ihlen, "Cardiac monitoring using transducers attached directly to the heart", in *2008 IEEE Ultrasonics Symposium*, Nov. 2008, pp. 749–752.

[20] A. Espinoza, P. S. Halvorsen, L. Hoff, H. Skulstad, E. Fosse, H. Ihlen, and T. Edvardsen, "Detecting myocardial ischaemia using miniature ultrasonic transducers–a feasibility study in a porcine model", *Eur J Cardiothorac Surg*, vol. 37, no. 1, pp. 119–126, Jan. 2010.

[21] A. Espinoza, P. S. Halvorsen, H. Skulstad, R. Lundblad, J. F. Bugge, L. Hoff, E. Fosse, and T. Edvardsen, "Automated detection of myocardial ischaemia by epicardial miniature ultrasound transducers–a novel tool for patient monitoring during cardiac surgery", *Eur J Cardiothorac Surg*, vol. 39, no. 1, pp. 53–59, Jan. 2011.

[22] T. T. Nguyen, A. W. Espinoza, E. W. Remme, J. D'hooge, and L. Hoff, "Transmural myocardial strain distribution measured at high spatial and temporal resolution", in *2011 IEEE International Ultrasonics Symposium*, Oct. 2011, pp. 696–699.

[23] O. Bonnefous and P. Pesque, "Time domain formulation of pulse-doppler ultrasound and blood velocity estimation by cross correlation", *Ultrasonic imaging*, vol. 8, no. 2, pp. 73–85, 1986.

[24] A. P. Hoeks, T. G. Arts, P. J. Brands, and R. S. Reneman, "Comparison of the performance of the RF cross correlation and doppler autocorrelation technique to estimate the mean velocity of simulated ultrasound signals", *Ultrasound Med Biol*, vol. 19, no. 9, pp. 727–740, 1993.

[25] G. F. Pinton, J. J. Dahl, and G. E. Trahey, "Rapid tracking of small displacements with ultrasound", *IEEE transactions on ultrasonics, ferroelectrics, and frequency control*, vol. 53, no. 6, pp. 1103–1117, 2006.

[26] J. A. Jensen, *Estimation of Blood Velocities Using Ultrasound: A Signal Processing Approach*. Cambridge University Press, Mar. 29, 1996, 344 pp., Google-Books-ID: 2pZOAAAAIAAJ.

[27] J. G. Miller, J. E. Perez, S. A. Wickline, S. L. Baldwin, B. Barzilai, V. Davila-Roman, R. J. Fedewa, A. E. Finch-Johnston, C. S. Hall, S. M. Handley, F. D. Hockett, M. R. Holland, A. Kovacs, G. M. Lanza, S. H. Lewis, J. N. Marsh, J. Mobley, D. E. Sosnovik, R. L. Trousil, K. D. Wallace, and K. R. Waters, "Backscatter imaging and myocardial tissue characterization", in *1998 IEEE Ultrasonics Symposium. Proceedings (Cat. No. 98CH36102)*, vol. 2, 1998, 1373–1383 vol.2.

[28] C. Jia, R. Olafsson, S.-W. Huang, T. J. Kolias, K. Kim, J. M. Rubin, H. Xie, and M. O'Donnell, "Comparison of 2-d speckle tracking and tissue doppler imaging in an isolated rabbit heart model", *IEEE Trans Ultrason Ferroelectr Freq Control*, vol. 57, no. 11, pp. 2491–2502, Nov. 2010.

[29] S. Hyler, S. E. Pischke, P. S. Halvorsen, A. Espinoza, J. Bergsland, T. I. Tønnessen, E. Fosse, and H. Skulstad, "Continuous monitoring of regional function by a miniaturized ultrasound transducer allows early quantification of low-grade myocardial ischemia", *Journal of the American Society of Echocardiography*, vol. 28, no. 4, pp. 486–494, 2015.

[30] E. Commission *et al.*, "Directive 2010/63/eu of the european parliament and of the council of 22 september 2010 on the protection of animals used for scientific purposes", *Off J Eur Union*, vol. 276, pp. 33–79, 2010.

[31] I. Céspedes, Y. Huang, J. Ophir, and S. Spratt, "Methods for estimation of subsample time delays of digitized echo signals", *Ultrason Imaging*, vol. 17, no. 2, pp. 142–171, Apr. 1995.

[32] T. T. Nguyen, A. W. Espinoza, S. Hyler, E. W. Remme, J. D'hooge, and L. Hoff, "Velocity resolution improvement for high temporal resolution ultrasonic transducer", in *2017 IEEE International Ultrasonics Symposium (IUS)*, IEEE, 2017, pp. 1–4.

[33] P. M. Embree, *The accurate ultrasonic measurement of the volume flow of blood by time domain corelation.* PhD thesis, Dept. Elec. Eng., University of Illinois, Urbana, I11., 1986.

[34] S. G. Foster, P. M. Embree, and W. D. O'Brien, "Flow velocity profile via time-domain correlation: Error analysis and computer simulation", *IEEE transactions on ultrasonics, ferroelectrics, and frequency control*, vol. 37, no. 3, pp. 164–175, 1990.

[35] J. A. Jensen and N. B. Svendsen, "Calculation of pressure fields from arbitrarily shaped, apodized, and excited ultrasound transducers", *IEEE transactions on ultrasonics, ferroelectrics, and frequency control*, vol. 39, no. 2, pp. 262–267, 1992.

[36] J. A. Jensen, "Field: A program for simulating ultrasound systems", in *10th Nordicbaltic Conference on Biomedical Imaging, Vol.4, Supplement 1, Part 1: 351–353*, Citeseer, 1996.

[37] F. Kremer, H. F. Choi, P. Claus, and J. D'hooge, "2d myocardial strain assessment in the mouse: A comparison between a synthetic lateral phase approach and block-matching using computer simulation", *Ultrasonics*, vol. 52, no. 7, pp. 936–942, 2012.

[38] E. Waks, J. L. Prince, and A. S. Douglas, "Cardiac motion simulator for tagged mri", in *Proceedings of the workshop on mathematical methods in biomedical image analysis*, IEEE, 1996, pp. 182–191.

[39] T. T. Nguyen, A. W. Espinoza, S. Hyler, E. W. Remme, J. D'hooge, and L. Hoff, "Effect of myocardial perfusion on end-systolic radial strain at the apex", in *2012 IEEE International Ultrasonics Symposium*, IEEE, 2012, pp. 1–4.

[40] ——, "Estimating regional myocardial contraction using miniature transducers on the epicardium", *Ultrasound in medicine & biology*, vol. 45, no. 11, pp. 2958–2969, 2019.

[41] ——, "Transmural strain distribution across the cardiac wall and its dependency on measurement site", in *2012 IEEE International Ultrasonics Symposium*, IEEE, 2012, pp. 1–4.

Paper A

Estimating Regional Myocardial Contraction Using Miniature Transducers on the Epicardium

Thuy Thu Nguyen[a], **Andreas W. Espinoza**[b,c], **Stefan Hyler**[b], **Espen W. Remme**[d], **Jan D'hooge**[e], **Lars Hoff**[a]

[a]Dept. of Microsystems, University of South-Eastern Norway, Horten, Norway.

[b]The Intervention Centre and [c]Dept.of Anaesthesiology, Oslo University Hospital, Rikshospitalet, Oslo, Norway.

[d]Institute for Surgical Research, Oslo University Hospital, Rikshospitalet, Oslo, Norway.

[e]Lab. on Cardiovascular Imaging Dynamics, Dept. of Cardiovascular Diseases, Catholic University of Leuven, Leuven, Belgium.

This paper has been accepted for publishing in Ultrasound in Medicine and Biology.

Paper B

Myocardial strain measured by epicardial transducers – comparison between velocity estimators

Thuy Thu Nguyen[a], **Andreas W. Espinoza**[b,c], **Stefan Hyler**[b], **Espen W. Remme**[d], **Jan D'hooge**[e], **Lars Hoff**[a]

[a]Dept. of Microsystems, University of South-Eastern Norway, Horten, Norway.

[b]The Intervention Centre and [c]Dept.of Anaesthesiology, Oslo University Hospital, Rikshospitalet, Oslo, Norway.

[d]Institute for Surgical Research, Oslo University Hospital, Rikshospitalet, Oslo, Norway.

[e]Lab. on Cardiovascular Imaging Dynamics, Dept. of Cardiovascular Diseases, Catholic University of Leuven, Leuven, Belgium.

This paper is under internal revision and will be submitted to Ultrasound in Medicine and Biology soon. The paper published in the IEEE International Ultrasonics Symposium Proceedings 2017 [32] is covered by this paper.

Paper C

Transmural Myocardial Strain Distribution Measured at High Spatial and Temporal Resolution

Thuy Thu Nguyen[a], **Andreas W. Espinoza**[b,c], **Stefan Hyler**[b], **Espen W. Remme**[d], **Jan D'hooge**[e], **Lars Hoff**[a]

[a]Dept. of Microsystems, University of South-Eastern Norway, Horten, Norway.

[b]The Intervention Centre and [c]Dept.of Anaesthesiology, Oslo University Hospital, Rikshospitalet, Oslo, Norway.

[d]Institute for Surgical Research, Oslo University Hospital, Rikshospitalet, Oslo, Norway.

[e]Lab. on Cardiovascular Imaging Dynamics, Dept. of Cardiovascular Diseases, Catholic University of Leuven, Leuven, Belgium.

This paper has been pusblished in the IEEE International Ultrasonics Syposium Proceedings 2011, pp. 696-699.

Paper D

Transmural Strain Distribution Across the Cardiac Wall and Its Dependency on Measurement Site

Thuy Thu Nguyen[a], **Andreas W. Espinoza**[b,c], **Stefan Hyler**[b], **Espen W. Remme**[d], **Jan D'hooge**[e], **Lars Hoff**[a]

[a]Dept. of Microsystems, University of South-Eastern Norway, Horten, Norway.

[b]The Intervention Centre and [c]Dept.of Anaesthesiology, Oslo University Hospital, Rikshospitalet, Oslo, Norway.

[d]Institute for Surgical Research, Oslo University Hospital, Rikshospitalet, Oslo, Norway.

[e]Lab. on Cardiovascular Imaging & Dynamics, Dept. of Cardiovascular Diseases, Catholic University of Leuven, Leuven, Belgium.

This paper has been pusblished in the IEEE International Ultrasonics Syposium Proceedings 2012, pp. 1-4.

Paper E

Effect Of Myocardial Perfusion on End-systolic Radial Strain at the Apex

Thuy Thu Nguyen[a], **Andreas W. Espinoza**[b,c], **Stefan Hyler**[b], **Espen W. Remme**[d], **Jan D'hooge**[e], **Lars Hoff**[a]

[a]Dept. of Microsystems, University of South-Eastern Norway, Horten, Norway.

[b]The Intervention Centre and [c]Dept.of Anaesthesiology, Oslo University Hospital, Rikshospitalet, Oslo, Norway.

[d]Institute for Surgical Research, Oslo University Hospital, Rikshospitalet, Oslo, Norway.

[e]Lab. on Cardiovascular Imaging & Dynamics, Dept. of Cardiovascular Diseases, Catholic University of Leuven, Leuven, Belgium.

This paper has been pusblished in the IEEE International Ultrasonics Syposium Proceedings 2012, pp. 1-4.

Paper F

Implementation and Use of the Software. Data Processing Algorithms and Simulation of Myocardial Motion

Thuy Thu Nguyen[a], **Lars Hoff**[a]

[a]Dept. of Microsystems, University of South-Eastern Norway, Horten, Norway.

This paper has been prepared as a report for internal use.

Doctoral dissertation no. 68
2020
—

Layer-specific strain and strain rate: Estimation using miniature transducers attached to the epicardium

Dissertation for the degree of PhD

Thuy Thu Nguyen

—

ISBN: 978-82-7860-429-8 (print)
ISBN: 978-82-7860-430-4 (online)

usn.no